CHALMERS

Changes of hydraulic properties in the rock close to a tunnel due to excavation and grouting

- A conceptual model and a case study

Master of Science Thesis in the Master's Programme Geo and Water Engineering

EMIL JOHANSSON & JOAKIM WALLGREN

Department of Civil and Environmental Engineering
Division of GeoEngineering
CHALMERS UNIVERSITY OF TECHNOLOGY
Göteborg, Sweden 2011
Master's Thesis 2011:2

Changes of hydraulic properties in the rock close to a tunnel due to excavation and grouting

- A conceptual model and a case study

Master of Science Thesis in the Master's Programme Geo and Water Engineering

EMIL JOHANSSON & JOAKIM WALLGREN

Department of Civil and Environmental Engineering
Division of GeoEngineering
CHALMERS UNIVERSITY OF TECHNOLOGY

Gothenburg, Sweden 2011

Changes of hydraulic properties in the rock close to a tunnel due to excavation and grouting
- A conceptual model and a case study
Master of Science Thesis in the Master's Programme Geo and Water Engineering
EMIL JOHANSSON & JOAKIM WALLGREN

Department of Civil and Environmental Engineering
Division of GeoEngineering
Chalmers University of Technology
SE-412 96 Göteborg
Sweden
Telephone: + 46 (0)31-772 1000

Cover: 3D-model of the TASS-tunnel and its fracture orientation

Changes of hydraulic properties in the rock close to a tunnel due to excavation and grouting

- A conceptual model and a case study

Master of Science Thesis in the Master's

EMIL JOHANSSON & JOAKIM WALLGREN

Department of Civil and Environmental Engineering
Division of GeoEngineering
Chalmers University of Technology

ABSTRACT

In tunnel construction and grouting of rock, there is always a risk of normal deformations or shear deformations of existing fractures. If the grouting pressure is too high or the fractures are orientated in a not preferable direction to the tunnel front or tunnel wall/floor, deformations may occur. This can lead to hydraulic changes, which can have a large impact on the tunnel.

A literature study has been made in order to identify and understand relations between different rock mechanical- and hydraulic properties. The created conceptual model is then applied on a real case scenario, the TASS-tunnel in Äspö Hard Rock Laboratory (HRL). Data from different field tests in the TASS-tunnel has been evaluated and been used as a base for evaluations and comparison.

It is the vertical fractures going perpendicular to the tunnel that is most likely to deform, due to shear stresses. Thanks to the preferable fracture orientation and the effective principal stresses that occur, there will only be normal deformations close to the tunnel contour. What grade of deformation that occurs is not possible to see, but data from the different grouting stages indicates that deformations and changes of hydraulic properties really occur.

Shear deformations will most likely occur in the vertical fracture set going perpendicular to the tunnel with a deviation of 10-40° to the largest principal stress σ_1.

Key words: hydraulic properties, normal deformation, shear deformation, pre-grouting,   post-grouting, rock stresses

Förändringar av de hydrauliska egenskaperna i berg nära tunnlar vid utgrävning och injektering
- En konceptuell modell och fallstudie
Examensarbete inom Masterprogrammet Geo and Water Engineering
EMIL JOHANSSON & JOAKIM WALLGREN
Institutionen för bygg- och miljöteknik
Avdelningen för Geologi och Geoteknik
Chalmers tekniska högskola

SAMMANFATTNING

Vid tunnelbyggande i berg och injektering finns alltid risk för normaldeformering eller skjuvdeformering av befintliga sprickor. Om injekteringstrycket är för högt eller sprickorna ligger i en ofördelaktig riktning gentemot tunnelfronten, eller tunnelvägg/golv, kan deformationer ske. Detta kan i sin tur ge upphov till stora hydrauliska förändringar, vilket kan ha stor inverkan på tunneln.

En litteraturstudie har genomförts för att identifiera och förstå samband mellan olika bergsmekaniska- och hydrauliska egenskaper. Den framställda konceptuella modellen har sedan applicerats på en riktig tunnel, TASS-tunneln i Äspö:s bergslaboratorie. Data från olika försök i TASS-tunneln har utvärderats och använts som underlag för utvärdering och jämförelse.

Det är de vertikala sprickorna som går vinkelrätt mot tunneln som är de som mest troligen kommer deformeras, skjuvdeformeras. Tack vare den fördelaktiga sprickorienteringen och de principiella effektivspänningar som råder kommer bara normaldeformation ske nära tunnelkonturen. Vilken grad av deformation som råder går inte att se, men mätdata från de olika injekteringsstegen tyder på att deformation och ändrade hydrauliska egenskaper verkligen sker.

Det är mest troligt att skjuvdeformationen kommer ske i det vertikala sprickset som går vinkelrätt mot tunnelriktiningen med en avvikelse på 10-40° från den största principiella spänningen σ_1.

Nyckelord: hydrauliska egenskaper, normaldeformation, skjuvdeformation, förinjektering, efterinjektering, bergsspänningar

Contents

List of appendices

Preface

Excavation and grouting of tunnels influence the stresses in rock which in turn may influence the hydraulic properties. The starting point in this thesis is a simplified description of the fractured rock with the objective to handle this issue. The description includes in-situ rock stresses, fracture (set) orientation, friction angle, and tunnel geometry. Estimates of rock stresses are compared to water- and grouting pressures where low (no) effective stress is assumed to be an indication of fracture deformation.

This work is a first step in developing a method for compilation, presentation and analyses of hydromechanical issues when constructing tunnels in rock and could be a complement to methods where a lot of information is reduced to single numbers (like in the commonly used rock classification systems).

Göteborg, March, 2011

Åsa Fransson

Preface

The purpose with this master thesis was to do a literature study and to investigate changes of hydraulic properties in a rock, close to a tunnel due to grouting and excavation. The master thesis was carried out at the Department of Civil and Environmental Engineering, Division of GeoEngineering, Chalmers University of Technology, Sweden, during the year 2010.

We wish to thank Åsa Fransson, our supervisor and Gunnar Gustafson for guidance and help with the thesis. We also would like to thank our opponents Tom Karlsson and Jonas Tallberg for valuable comments. Peter Hedborg also deserves a great thank for all the help with our computers.

Finally we would like to thank the Division of GeoEngineering for letting us do our master thesis for them and providing us with an office.

Gothenburg January 2011

Emil Johansson   Joakim Wallgren

Notations

Roman upper case letters

D	[m]	Depth
E	[Pa]	E-modulus
Q	[m³/s]	Fluid flow
I_{max}	[m]	Maximum penetration length for grouting agent
T	[m²/s]	Transmissivity

Roman lower case letters

a	[m]	Radius of a circular opening in Kirsch equations
b	[m]	Fracture aperture
b_h	[m]	Hydraulic aperture
dh	[m]	Change of hydraulic head
g	[m/s²]	Acceleration due to gravity
k	[-]	Ratio of horizontal stress and vertical stress in Kirsch equations
k_n	[Pa/m]	Fracture normal stiffness
p	[Pa]	Fluid pressure
p_{slip}	[Pa]	Fluid pressure causing shear deformation
p_g	[Pa]	Grouting pressure
p_w	[Pa]	Water pressure
r	[m]	Radius to the centre of a circular opening in Kirsch equations

Greek upper case letters

Δp	[Pa]	Grouting overpressure
Δu_n	[m]	Fracture normal deformation
$\Delta \sigma_n'$	[Pa]	Change in effective normal stress

Greek lower case letters

α	[°]	Angle between fracture plane and the largest principal stress
γ	[kg/m³]	Density
ε	[m]	Tension
μ	[Pa·s]	Viscosity
μ_f	[-]	Mobilized friction coefficient
ρ_w	[kg/m³]	Density of water
σ	[Pa]	Stress
σ'	[Pa]	Effective stress
σ_n'	[Pa]	Effective normal stress
σ_1	[Pa]	Largest principal stress

σ_2	[Pa]	Intermediate principal stress
σ_3	[Pa]	Smallest principal stress
σ_H	[Pa]	Largest horizontal stress
σ_h	[Pa]	Smallest horizontal stress
σ_n	[Pa]	Normal stress
σ_r	[Pa]	Radial stress around a circular opening
σ_θ	[Pa]	Tangential stress around a circular opening
σ_v	[Pa]	Vertical stress
σ_x	[Pa]	Horizontal stress in Kirsch equations
σ_z	[Pa]	Vertical stress in Kirsch equations
τ	[Pa]	Shear stress
τ_0	[Pa]	Yield strength
τ_{max}	[Pa]	Maximum shear stress
τ'_{max}	[Pa]	Effective maximum shear stress
$\tau_{r\theta}$	[Pa]	Shear stress around a circular opening in Kirsch equations
ϕ	[°]	Friction angle

Abbreviations

HRL	Hard rock laboratory
RQD	Rock quality designation
SKB	Svensk Kärnbränslehantering AB
TBM	Tunnel boring machine

1 Introduction

1.1 Background

Humans have always been fascinated in advanced infrastructure and tunnels are no exception. Tunnels are nowadays a common and very important type of structure in order to create safe and time saving solutions. When excavating the rock, by drill and blast or TBM (tunnel boring machine), the ground water level in the nearby area is lowered. This is often due to inflow of ground water into the tunnel. That could lead to a reduced bearing capacity in the surrounding ground and in the long run settlements or dry up wells. In urban areas it is of big importance to avoid settlements, particularly when comparing to rural areas where the restrictions are usually much lower. This is because of denser infrastructural presence. To avoid water leaking into the tunnel grouting is performed. The inflow requirements change depending on where the tunnel is situated. During excavation in hard rock there will be deformation and stress changes in the nearby rock. The deformation will cause geometric changes of the fractures which may reduce the effect of the grouting performed. This will lead to changes of the hydraulic properties when the excavation has taken place under the ground water table. The extent of the hydraulic changes is connected to the fracture intensity and stress changes in the rock.

Water leaking into the tunnel during the excavation stage could lead to different problems depending on depth, location and time of the year. During cold periods the water leaking into the tunnel from the ceiling may cause icicles, which could damage the vehicles operating in the tunnel.

Another problem related to the ingress of ground water is that pumps may be needed to be able to operate in the tunnel. This is time consuming and uncomfortable working climate during the excavations phase and leads to high pumping costs in the operation phase.

1.2 Purpose

The purpose with the report is to increase the understanding of the relation between the geology, hydraulic properties and rock mechanics and how these subjects affect the ground water inflow in a tunnel due to excavation and grouting. The purpose is to create a conceptual model and a case study that highlights relevant questions related to these subjects and relations between them.

1.3 Problem definition

The work will result in a conceptual model that will be applied to the case study. By applying the conceptual model on the case study the following questions are highlighted, discussed and answered:

- Is it possible to indicate impacts on the water-bearing fracture system caused by excavation and grouting? If there are impacts indicated can they affect the fractures' ability to conduct water?

- How does change of rock stresses due to excavations affect surrounding ground water-bearing fractures? If there is any significant impact on the fractures is it possible it will lead to changes in ground water inflow?

- What impact(s) does the excavation and grouting have on different fracture orientations in relation to the excavation?

- What impact(s) does pre- and post-grouting have on the hydraulic properties in fractures? May the grouting pressure required to seal intended fractures cause deformations of other fractures and change the hydraulic properties?

1.4   Delimitation

The report highlights the theoretical relations between geology, hydraulic properties in the rock and rock mechanics when performing excavation and pre- and post-grouting. The conceptual model will be used as a basis for qualitative analysis of the TASS-tunnel at Äspö Hard Rock Laboratory (HRL). The calculations regarding the shear deformations are assuming a solid rock and no excavation performed.

1.5   Method

First of all a literature study has been made in order to compile knowledge regarding the geology, hydraulic properties and rock mechanics and the relations between these subjects. Chapters 2-7 present the elementary facts and theories about these subjects and how they are related.

With these chapters as a basis a conceptual model is created and possible scenarios and behaviour of the hydraulic properties due to excavation and pre- and post-grouting are presented in chapter 8.

The conceptual model is applied to a real case scenario, the TASS-tunnel at Äspö HRL. Simplified descriptions of the fracture system and rock stresses have been made and are presented in chapter 9. Based on the description, changes of hydraulic properties in the rock close to the tunnel due to excavation and grouting are discussed and finally data from the case study has been used to see if the potential changes could be confirmed.

2   Conceptual models in general

The purpose with the Master Thesis is to create a conceptual model that treats changes of hydraulic properties in the rock close to a tunnel due to excavation and grouting. Before the conceptual model is created it is important to describe and evaluate what a conceptual model is.

There are different descriptions of what a conceptual model is and what it is used for. One common description is that a conceptual model is the relation between what we measure and see and the understanding of the physical system. Models are used to understand, to analyze and to predict. Therefore a conceptual model could be a really important tool in many different areas e.g. environment, economy and health. A model should also be up-to-date which means that the input could change over time which could lead to another output. It is also important to realize that models are not always reality. It could sometimes be better to model how things cannot be rather than how they are (Gustafson 2007).

According to Rhén et al. (2003) a conceptual model can be defined as a model that describes the geometry. It could also be a structural framework where a problem should be solved, the size of the modelling volume (scale), the equations which lead the process forward and boundary conditions (Rhén et al. 2003).

Conceptual models are mental images of something real e.g. systems, processes or objects. The conceptual model is something that is used to try new ideas and has an important role in development. Therefore a conceptual model could be a personal opinion or thought, but the more evaluation of data and theories put behind it, the more reliable the model is.

Rhén's definition of a conceptual model is the one most similar to the one used in the report. Parameters of interest for our aim has been chosen and set as boundaries. The conceptual model in this report is a suggested way of evaluating and adopting a created tool in order to see the changes of hydraulic properties, fractures and stresses in rock during tunnel processing.

The conceptual model that is created in this Master Thesis can be a guide and help to identify potential problems about water inflow in a tunnel due to excavation and grouting. The assumptions and evaluation that are made come from the authors of the Master Thesis and is backed up by essential information after literature studies. By applying the conceptual model on a real scenario the models relevance can be evaluated and if necessarily be improved.

3 The rock

This chapter treats different rock types and how they are created. This could be of importance when evaluating fractures and hydraulic properties in the bedrock and potential problems.

There are commonly three main groups of different rock types – sedimentary, metamorphic and igneous rocks. There are many different rock types in each group with different properties. Each and every one of the rock types behaves differently when being exposed to stresses.

3.1 Sedimentary rock

One of the three main rock types is sedimentary rock. Sedimentary rock could be divided into three different subgroups, clastic, organic and chemical sedimentation, all with different characteristics. General for all sedimentary rock is that it is created by material stripped away by erosion and water. The material is carried away by streams and glaciers into rivers, and some into the ocean (Goodman 1993). Wind could also carry material. When the wind or water cannot transport the particles any longer they fall down to the ground or bottom and become deposited.

According to (Goodman 1993) bedding and bedding surfaces are the most important structural features of sedimentary rocks. They are usually, but not always, conspicuous and influential for the properties of sedimentary rock masses.

Clastic sedimentation is when eroded material – mostly quartz and clays – are gathered together creating a layer of material. The layers often consist of many different grain sizes and material and the word *clast* is used to define that many different materials are gathered together. After the deposition the layers start turning into rock and that process is called diagenesis. The first step of the process is compaction which occurs when the overlaying material is increasing. An increased pressure from the overlaying material is forcing the grains in the lower layers together which reduces the pore space and eliminates some of the contained water. The next step is cementation and that is when the individual particles start to bind together. After a long time the particles become so hard that a new rock is created. If the compaction is too high it might cause recrystallization of the minerals which would make the rocks even harder (Nelson 2003).

Depending on what kind of grain sizes that occur in each layer, the texture of a clastic sedimentary rock could differ as shown in Figure 3.1. The texture differs due to density and the energy of the transport medium. Transportation medium with high energy can carry particles with varying grain size and therefore are those sediments often poorly sorted. Transport mediums with lower energy are bound to carry smaller particles and therefore are those sediments well sorted (Nelson 2003). The texture of the sediment is a good way to understand how the sediment was created.
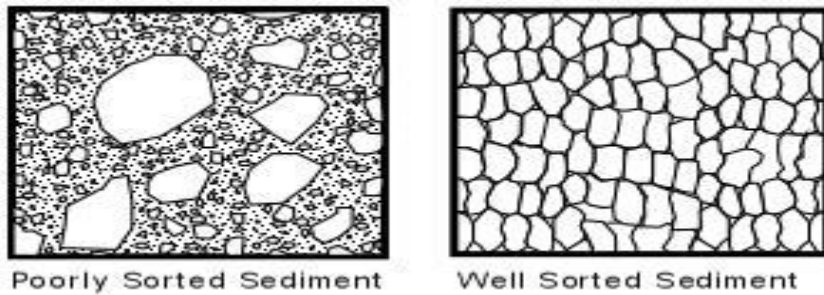
Poorly Sorted Sediment   Well Sorted Sediment

Figure 3.1   Different textures of clastic sedimentary rock (Nelson 2003).

During the transportation, by wind or water, the grains can be reduced in size due to abrasion. That could lead to a rounding off of the sharp edges of the grains. Figure 3.2 below show the process:
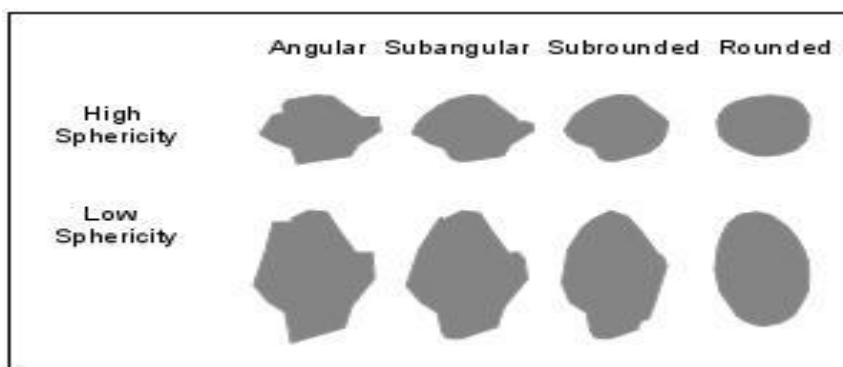

Figure 3.2   Different types of rounded grain (Nelson 2003).

Another type of sedimentation is the organic one which occurs when microscopic organisms and plankton build shells out of the dissolved calcium and carbonate or silica in the water. When the plankton dies they fall to the bottom where they accumulate in thick layers. Examples of organic created sedimentary rock are limestone and chert (Goodman 1993). It is common to find traces of fossils in limestone, and that is because the dead animals are trapped in sediments from other dead organisms and is being preserved. Therefore organic sedimentation can tell what kind of plants and animals that lived and died in that specific area. One has to know that the process is slow and takes time.

Chemical sedimentation occurs when the concentration of minerals in the water is increasing. The created rock during this process is limestone or dolomites, gypsum rock and rock salt. The minerals in chemical sedimentary rocks could be identified and therefore it is sometimes possible to say where the sedimentary rock comes from.

When sedimentary rock is created it is in layers. As mentioned earlier the process is time consuming and the sedimentary rock is clearly divided into different layers. The layers are not always horizontal. If there is long time between the different depositions wind and water could start tarring on the layers so when the next deposition occurs the layers could be cross bedded, as shown in Figure 3.3.
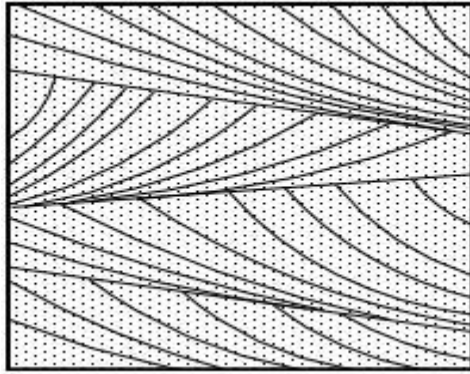
Figure 3.3   Wind and water may create cross bedded layers (Nelson 2003).

Sedimentary rock is not one of the preferred rock types when performing excavations. The rock often consists of different layers as in Figure 3.3 and one can assume a scenario like that would cause hydraulic problems. The borders between the layers would not be entirely sealed and is much weaker than the rest of the rock. Therefore fractures could disperse and the water bearing capacity would increase and the strength of the rock in total would decrease. All different kinds of sedimentary rock are created by the same principle so one can think that these kinds of problems would occur no matter if the rock is created by chemical, organic or clastic sedimentation.

3.2   Metamorphic rock

Metamorphism comes from the Greek where Meta means change and Morph means form. One can therefore say that metamorphism is changing of form. In a geological aspect it means the change in mineral assemblage and texture. This is due to pressure and temperature separately or together (Goodman 1993). Metamorphism occurs at temperatures higher than 200°C and pressure higher than 300 MPa. To be exposed for this high temperature and pressure the rock has to be buried deep in the Earth and that is possible due to tectonic processes such as subduction or continental collisions. When the pressure and temperature is so high that wet partial melting of the rock in question occurs the upper limit is reached. When the melting process begins it turns into an igneous process more than a metamorphic process. The process the rock is undergoing is called prograde metamorphism, the grade of metamorphism increases (Nelson, 2003).

Depending on temperature and pressure different states of metamorphism could occur. As can be seen in Figure 3.4 there are five different states with diagnesis as the state with lowest pressure and temperature and an igneous state when the temperature and pressure is high.
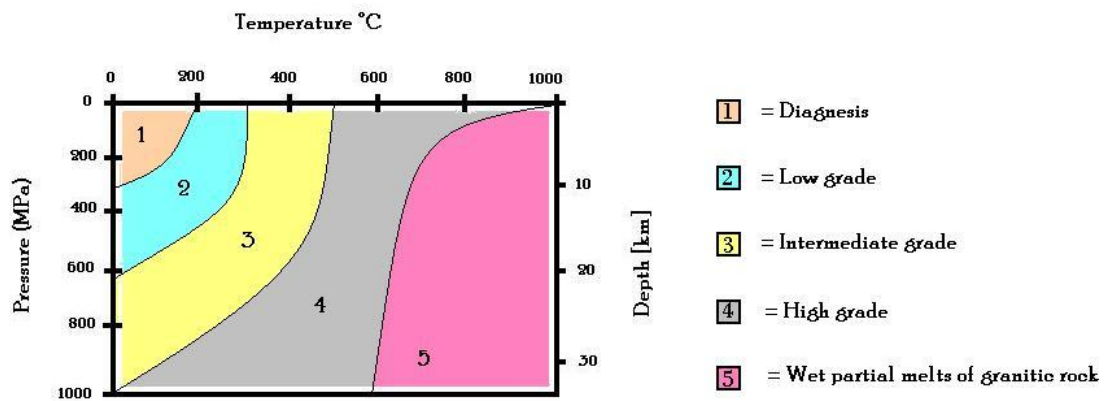
Figure 3.4   Shows the different pressure temperature of different metamorphosis (Modified from Nelson 2003).

One might think that the metamorphic process will be reversed if the temperature and pressure fall, due to tectonic uplift and erosion of overlying layers, and that the rock slowly will return to its original metamorphosed state. This process is called retrograde metamorphism and if it was common almost no metamorphic rock would occur at the earth's surface. Metamorphic rocks do often occur at the earth's surface so retrograde metamorphism is not very common (Nelson 2003). One reason for this is that chemical reactions take place more slowly when the temperature is lower. Another reason is that chemical reactions take place more rapidly when liquid is present, but the liquid is driven away during the prograde metamorphism so they will not be available to speed up the process during the retrograde metamorphism.

There are four different classes of metamorphism and cataclastic metamorphism is the first one. This process occurs due to mechanical deformation. It could be described as "when two bodies of rock slide past one another along a fault zone" (Nelson 2003). Due to the sliding the rock tends to crush and heat is generated by the friction between the sliding rocks.

Burial metamorphism is the second class of metamorphism and is taking place several hundreds of meter beneath the earth's surface where the temperature is more than 300°C. New minerals grow but the rock does not become metamorphosed. Burial metamorphism overlaps with diagenesis, see zone 1 in Figure 3.4, and grades into regional metamorphism.

Contact metamorphism, the third class of metamorphism, occurs together with igneous intrusions and is a result of high temperature. The process can be seen as a larger area where only a smaller inner part of the area is heated by the magma. This area is called metamorphic aureole. This core is metamorphosed but the surrounding area is not. Contact metamorphism occurs more often at shallow levels in the crust due to larger difference in temperature. At deeper levels the difference are smaller and therefore less contact metamorphism (Nelson 2003). Figure 3.5 shows the process.
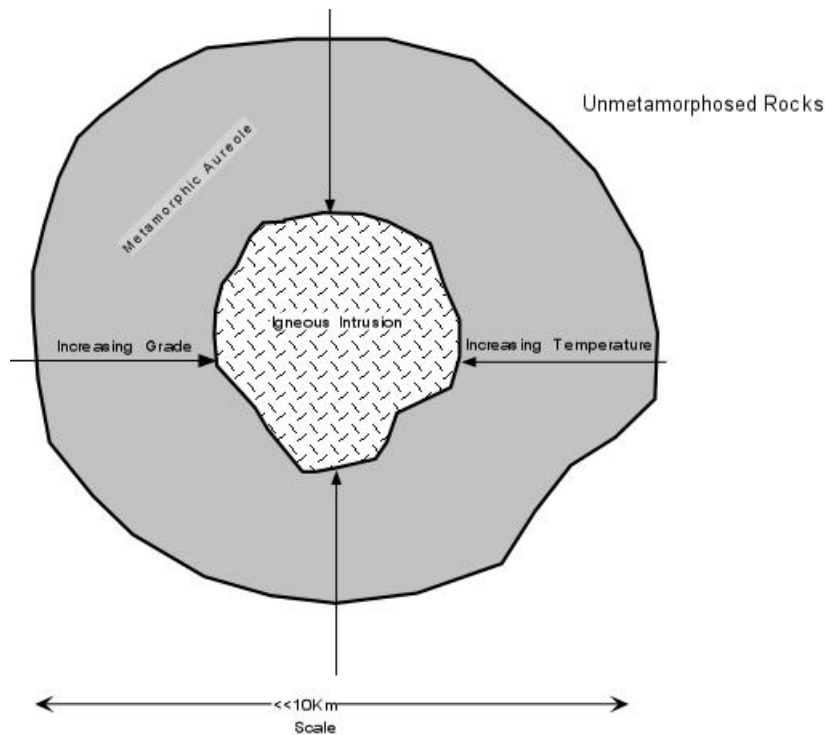
Figure 3.5   The principles of contact metamorphism (Earth Science, 2010).

The last type of metamorphism is the regional metamorphism which according to Nelson is a larger area that due to differential stresses has been subjected to a high degree of deformation. Usually the result of this is strongly foliated metamorphic rock. The stresses comes from tectonic forces like when two continental masses collide and therefore are regional metamorphic rocks often found in the core of mountain ranges or in eroded mountain ranges. The rocks are often pushed down to deeper levels due to the thickening of the crust from the foliation. This can be seen in Figure 3.6.
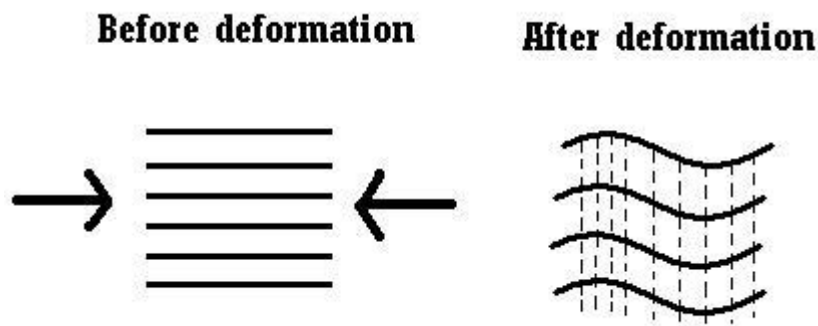

Figure 3.6   Regional metamorphism that foliates the rock (Modified from Nelson, 2003).

Regional metamorphism could affect the fracture systems heavily. Gneiss is created through regional metamorphism and in gneiss e.g. fractures often occur in sets with more or less well-defined preferred orientations. Often two or three steep fracture sets and a sub horizontal or a layer-parallel set are developed. The steep fractures orientation may be governed by the orientation of folds and other structures in the

rock mass. Therefore one can see that foliation in the rock mass can have an impact of the fracture system (Skjernaa & Jörgensen, 2004). Gneiss is a rock type characteristic for regional metamorphism so one can assume that these relations are the same in other rock types within the same metamorphism as well.

One feature of metamorphic rocks is a direction of parting, akin to bedding, which often maintains a general orientation for a considerable distance. This is called foliation and any foliated metamorphic rock will split much more easily along the foliation plane than in any other direction through the rock. That is why foliated rock could cause big problems during excavations (Goodman 1993).

3.3 Igneous rock

The third and last group of different rock types is igneous rocks. They are formed in two different ways. Either volcanic or extrusive which means that the rock type is formed when magma cools and crystallizes at the surface of the Earth or intrusive or plutonic which means that the rock type is formed when the magma crystallizes at depth in the Earth. Magma has less density than surrounding rocks and is therefore moving upward. If the magma makes it to the Earth surface it will crystallize there and form a volcanic or extrusive rock. If the magma crystallizes before it reaches the surface plutonic or intrusive rock types are formed. Depending on how the igneous rock is formed they differ from each other in texture and properties (Nelson 2003).

Extrusive and volcanic rock reaches the Earth's surface when they erupt from a vent. The eruption can be explosively or non-explosively. Non-explosively eruptions can be compared to water being pored over an already filled glass. The water flows over the edge of the glass and the same things happens with the lava flowing over the edge of the vent. The lava than crystallize at the surface when being cooled down. An explosively eruption occur when the pressure is too high in the vent. When the pressure becomes too high the lava is slung up in the air. Clouds of ashes and tephra create an eruption column which could reach up to 45 km into the atmosphere.

The intrusive or plutonic rock types are formed at deeper levels and can give rise to different types of formations. One type of formation formed at deeper level is dikes. They are often very small (< 20m wide) and show a discordant relationship to the rocks in which they intrude. Discordant means that the dikes do not follow the pre-existing structures. This could lead to problems when e.g. building tunnels and the tunnel front enters a dike zone. The dikes are often very fractured and exposed for stresses and therefore the dikes are often poor when it comes to hydraulic properties and bearing capacity.

Plutonic rock includes many particles with different crystal size and composition. The most of the igneous rock in the world are granitic in its composition. That means usually light-colored and trace of feldspar, quartz and mica, and pyroxene or amphibole. Granitic rocks often lack bedding but are often broken by several directions of planer fractures termed joints, especially sheet joints formed parallel to the land surface. Granitic rocks tend to hold high in situ stresses in the plane parallel to the sheet joints (Goodman 1993).

Batholiths are intrusive bodies which usually are so large that they seldom are exposed. Stocks are smaller bodies fed from the large batholiths beneath. The stocks

are usually a few kilometres wide while the batholiths beneath are 10s of kilometres (Nelson 2003). Figure 3.7, below, shows stock and batholiths.
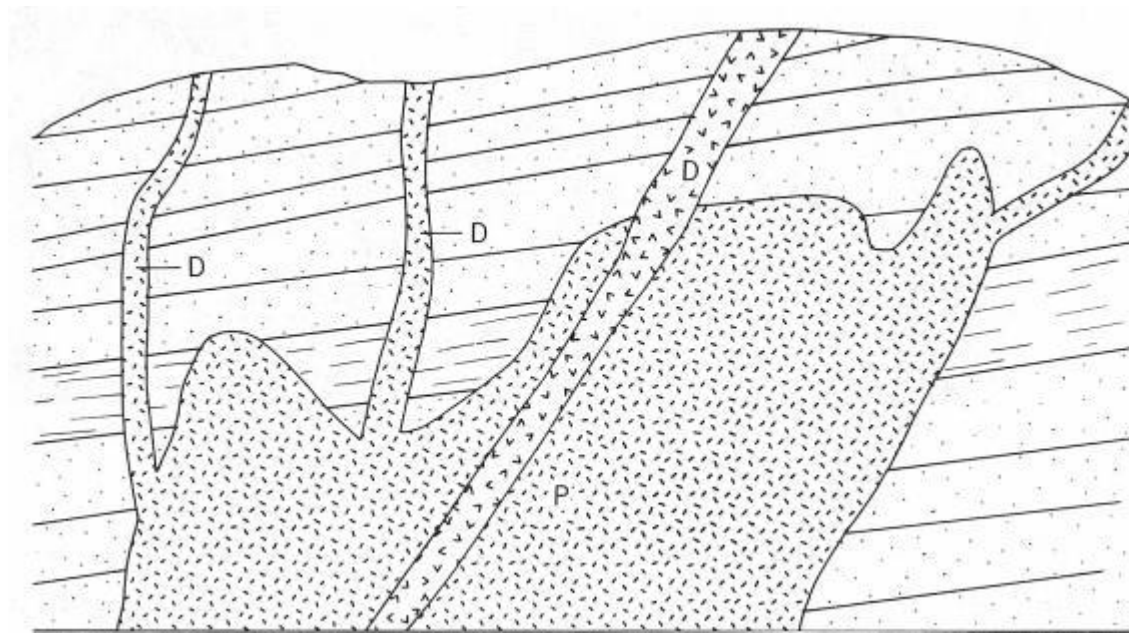

Figure 3.7   Picture of discordant igneous bodies where P is a pluton (intrusion) and D are dikes. (Goodman 1993).

Igneous rock could be very challenging when it comes to e.g. tunnel building, especially if the tunnel is crossing a zone with a lot of intrusions. The contact surface between the different rock types is often fractured and it could be hard to seal them even with grouting. This is because the rock close to the intrusions are less stable then the rest of the rock and small loose particles could get in the way for the grouting agent in the fractures.

3.4   E-modulus

The relationship between stress, σ, and tension, ε, is called E-modulus, *E*, and is expressed by Hooks law (Lindblom 2010):

$$E = \frac{\sigma}{\varepsilon} \qquad\qquad (3.1)$$

The E-modulus varies a lot in the different main rock types and could have a big impact on the rock properties. Figure 3.8 illustrate the elasticity modulus of some different rock types in each main rock group. The variations could be due to different age of the rock, different grade of weathering and different sets of minerals. There are also some rock types in each group that might have a higher E-modulus then the rest of the rock types in the same group but the figure below shows the general course of event. Noticeable is that the E-modulus values are the average value from the span that is presented in *Underground excavations in rock* (Hoek & Brown 1984). Seen in Figure 3.8, the sedimentary rocks do have the lowest E-modulus while the metamorphic rocks do have the highest E-modulus. Based on this it is understandable that sedimentary rock could be problem in e.g. tunnel excavations due to its relatively low E-modulus, while metamorphic rock are often more stabile and less problematic

to build in. The reason why a rock with low E-modulus is less preferable to excavate in is because large deformations may occur even when small stress redistributions take place.
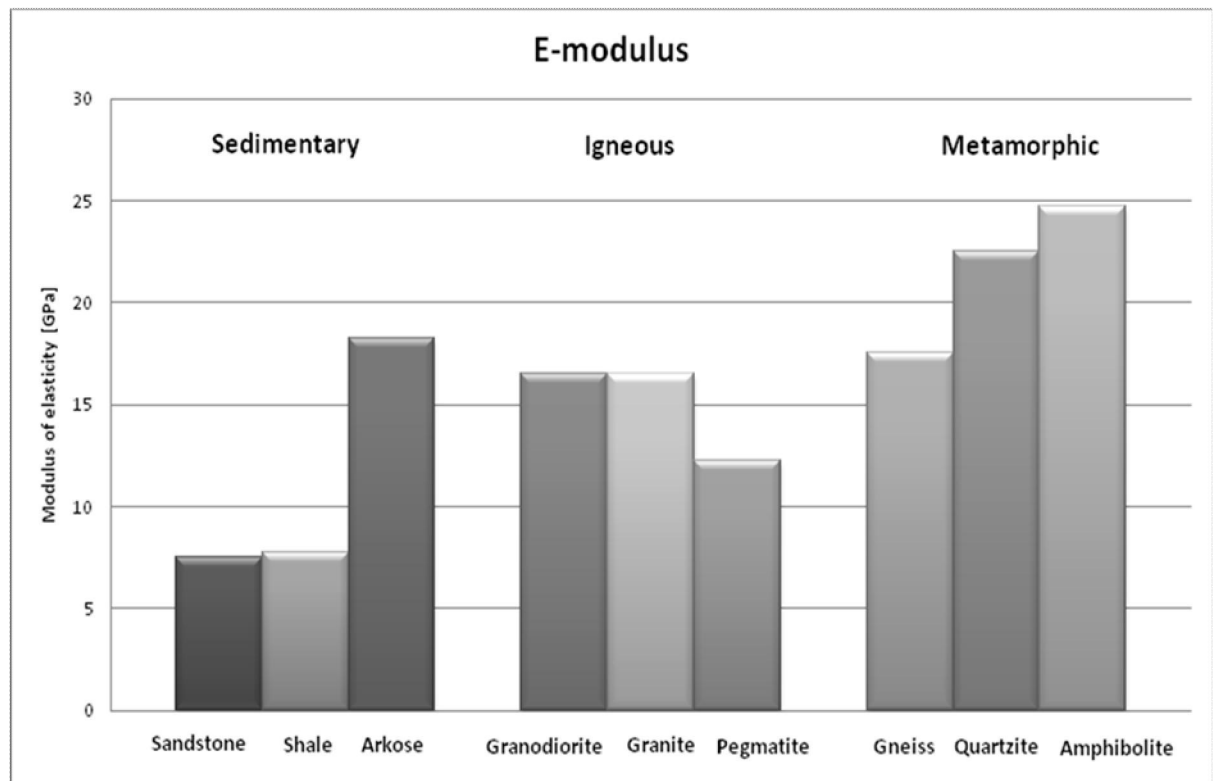

Figure 3.8   Average E-modulus for different rock types (Data from Hoek and Brown 1984).

Evaluation of the E-modulus is in reason done at an early stage of the building process. This is most easily done by field investigations and bore samples. The little amount of time and money the field tests take, in proportion to the entire project, could well be worth when an evaluation of the E-modulus could tell a lot about the rock properties and also what one can expect from the rest of the rock in the area.

4 Rock stresses

Before the excavation, when the rock is intact, there are in situ stresses, primary stresses, in the rock. The in situ stresses are mainly determined by the weight of the overlaying rock mass and the geological history of the rock. When excavating the tunnel the in situ stresses are rearranged into induced stresses which create a new stress pattern.

4.1 In situ stresses

Fracture orientations are a result of how the principal stresses have affected the bedrock mass during the years. Since the development and deformation of the bedrock that have been going on for millions of years and the stress pattern has changed there are large variations and complexity in the fracture systems. The bending and turning of stress direction have opened new fractures and healed others.

The stress matrix contains of three normal stresses in the diagonal, one in each direction in a x,y,z-coordinate system, see Figure 4.1. These normal stresses are directed perpendicular to the plane of the surface. The other elements pointed tangentially to the surface are shear forces. To describe how the stresses are orientated one uses the expressions trend and plunge. Trend describes the azimuth of the stress and plunge the dip of it. Usually a lot of measures are made to determine the stress plunge and dip and the mean values of these are used in the mean stress tensor. The result can be shown in a Schmidt net where the trend and plunge easily can be read (Martin et al. 2003).
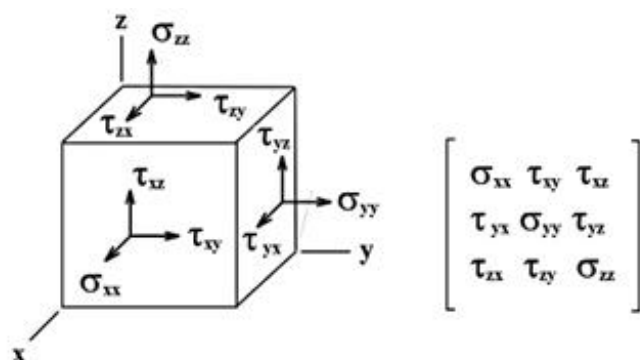
$$
\begin{bmatrix}
\sigma_{xx} & \tau_{xy} & \tau_{xz} \\
\tau_{yx} & \sigma_{yy} & \tau_{yz} \\
\tau_{zx} & \tau_{zy} & \sigma_{zz}
\end{bmatrix}
$$

Figure 4.1   The stress tensor consists of three principal stresses and two shear stresses at each face of the cube.

Stress data are recorded as σ_1, σ_2 and σ_3 where σ_1 is the largest stress and σ_3 the smallest ($\sigma_1 > \sigma_2 > \sigma_3$). The trend and plunge are recorded with the stress amplitude. The two largest principal stresses (σ_1 and σ_2) in Scandinavia are often within the plunge of 0-10° which means they are almost horizontal. The maximum horizontal stress, σ_H, and minimum horizontal stress, σ_h, can be interpreted as σ_1 and σ_2 respectively. The vertical stress, σ_v, is then synonymously used as σ_3 at shallow to medium depth. These circumstances for the Scandinavian shield make it possible to do these approximations for the stresses and should be handled with care in other projects (Martin et al. 2003).

Depending on the magnitude and orientation of the three normal stresses, different regimes of fractures are created in the bedrock, see Figure 4.2. The regimes differ in how the principal stresses (σ_1, σ_2, σ_3) are orientated. If the horizontal stresses, σ_H and σ_h, both are larger than the vertical stress the fracture orientation tend to be horizontal, called a thrust-faulting regime. When the second largest principal stress is not directed horizontally but vertically a strike-slip regime is present. In a strike-slip regime the vertical fractures perpendicular to the smallest principal stress, σ_3, are dominant. In the scenario when the largest principal stress, σ_1, is vertical a normal-faulting regime is present. This is also called an extensional regime and dominates of vertical fractures (Talbot & Sirat 2001, Schindler et al. 1998, Sibson 2004).
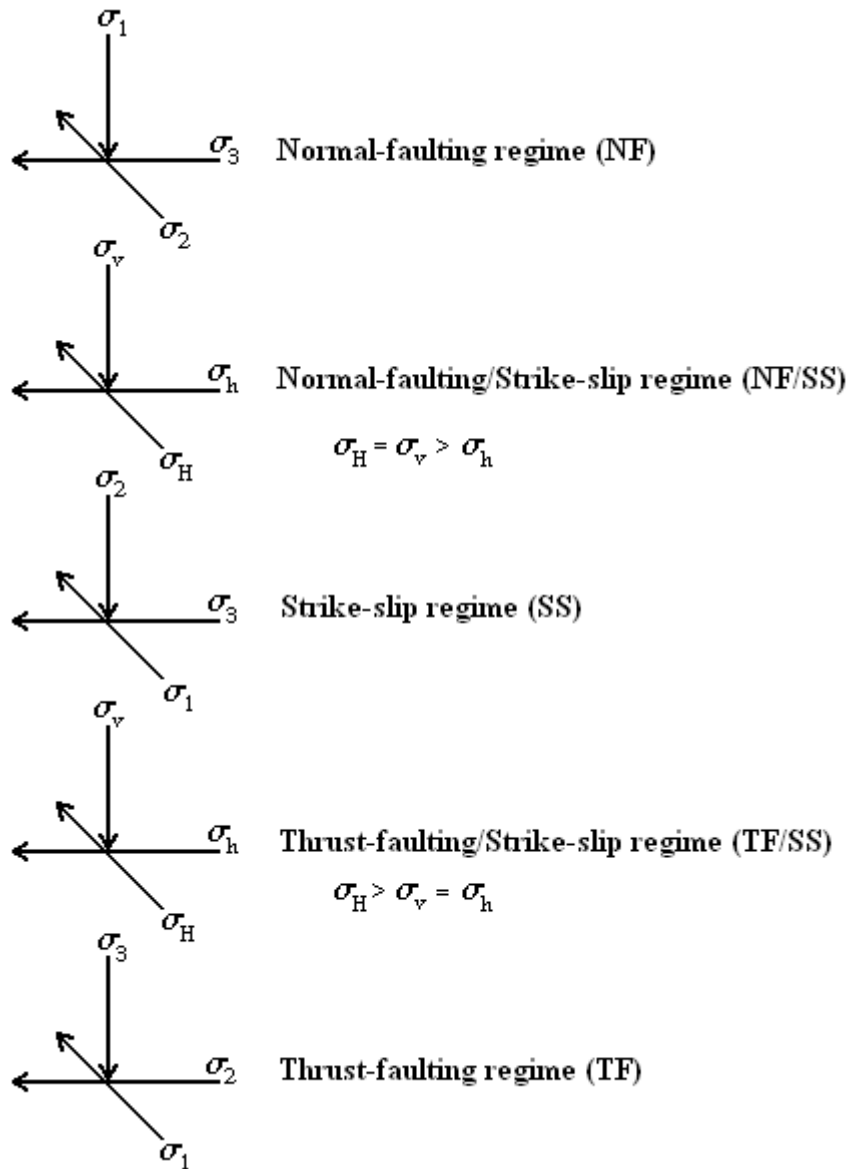

Figure 4.2   Different arrangement of the principal stresses determines what regime that is present in the rock (In situ conditions) (Schindler et al. 1998).

The vertical stress is highly dependent of the depth and is very often linear. The vertical stress is simple the density of the masses (γ) overlaying at a depth D. The

density of most rock masses is between 2500 and 3000 kg/m³ (25-30 kN/m³). This makes equation (4.1) usually used for estimating the vertical stresses.

$$\sigma_v = \gamma \cdot D \qquad (4.1)$$

There are cases where there can be deviation from the normal linear behaviour for the vertical stress. Faults may be one occurrence that may influence the so often linear behaviour of the vertical stress. In hilly and varying topography areas the vertical stress is more often deviated from the linear approximation than in flat areas. In these areas it is of great importance to investigate how the vertical stress varies by depth. In the Scandinavian bedrock the equation introduced above, equation (4.1), is not always practical to use since there are great differences. The result correlates with the equation at great depths but deviates at shallower depths (Martin et al. 2003).

4.2   Induced stresses

When excavating a tunnel the in situ stresses around the created opening are rearranged. The primary stresses (in situ) will be put into a new order, secondary stresses. The direction and magnitude of the secondary stresses is depending on the shape of the opening and properties of the primary stresses. The transformation from primary to secondary stresses causes deformations in the rock. Depending on the severity of the deformation it might be needed to support the rock by bolting or shotcrete. The support forces is categorized as a third link, tertiary stresses, and together with the primary and secondary stresses keeps the opening stable and the deformations small (Lindblom 2010).

The resulting elastic stress field around a circular hole created in an infinite plate when loading with two directional stresses, σ_z and σ_x, can be described by using Kirsch equations (Kirsch 1898):

$$\sigma_r = \frac{1}{2}\sigma_z \left[(1+k)\left(1-\frac{a^2}{r^2}\right) + (1-k)\left(1-4\frac{a^2}{r^2}+3\frac{a^4}{r^4}\right)\cos(2\theta) \right] \qquad (4.2)$$

$$\sigma_\theta = \frac{1}{2}\sigma_z \left[(1+k)\left(1+\frac{a^2}{r^2}\right) - (1-k)\left(1+3\frac{a^4}{r^4}\right)\cos(2\theta) \right] \qquad (4.3)$$

$$\tau_{r\theta} = \frac{1}{2}\sigma_z \left[-(1-k)\left(1+2\frac{a^2}{r^2}-3\frac{a^4}{r^4}\right)\sin(2\theta) \right] \qquad (4.4)$$

where k is the ratio between applied stresses:

$$k = \sigma_x / \sigma_z \qquad (4.5)$$

σ_r is the radial stress, σ_θ is the tangential stress, $\tau_{r\theta}$ is the shear stress, θ is the angle between the vertical centre line and the concerned point, a is the radius of the opening and r is the radius to the centre of the opening, see Figure 4.3. When a is equal to r (at the tunnel wall) the radial stress, σ_r, is equal to zero and the tangential stress equation can be reduced to (Lindblom 2010):

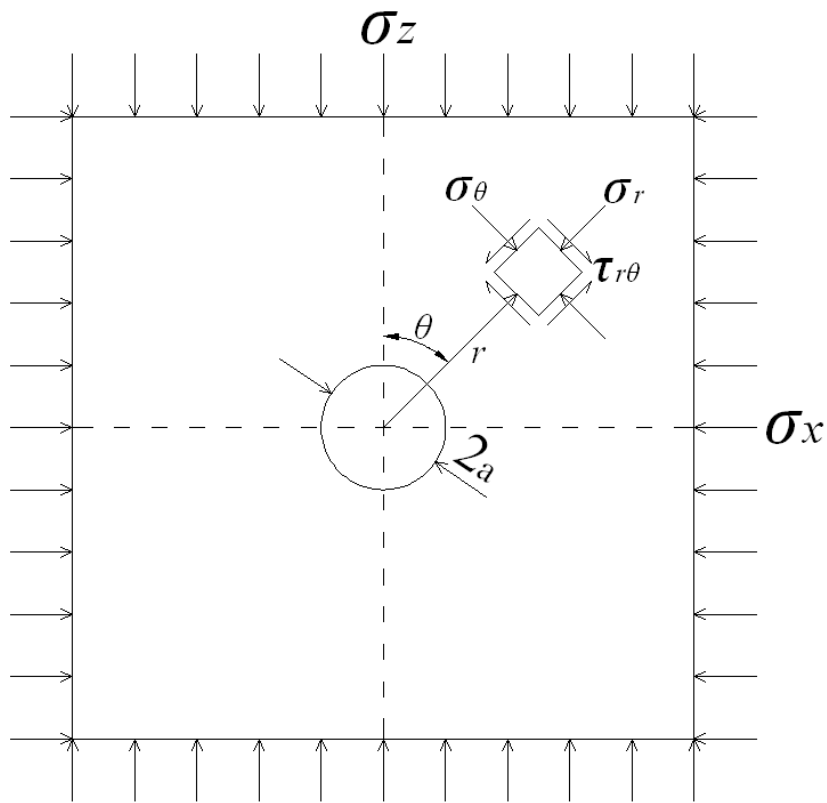$$\sigma_\theta = \sigma_z \left[(1+k) - (1-k) \cdot 2\cos(\theta) \right] \qquad (4.6)$$

Figure 4.3   Induced stresses, σ_r and σ_θ, are a result from biaxial loading an infinite, elastic plate with a circular opening (Lindblom 2010).

5   Fractures and fault zones

When the rock mass is exposed to stresses fractures are created. There are two different kinds of fractures, faults and joints. The origin of joints is when two rock faces have moved perpendicular away from each other and formed a fracture, a normal opening. Faults are generated when the two rock faces have slipped along each other and affected in a fracture, shearing. Fractures can consist by both these two origins, e.g. first faulted and then jointed and vice versa due to different stresses during long periods (Hobbs et al. 1976).

A ground water saturated fracture in the rock may deform due to changes of stresses in the rock or to changes of fluid pressure. Deformations caused by changes of stresses in the rock may take place when a tunnel in excavated. When the tunnel walls are grouted, either by pre- or post-grouting, there will be pressure changes in the fractures which may lead to deformation of the fracture. The rate of changes in stress and fluid pressure will affect the deformation magnitude of the fractures; more rapid changes will cause larger deformations (Rutqvist & Stephansson 2003).

The rock mass consists of solid rock and voids. The voids constitute the primary porosity of the rock mass and vary between the different rock types. The secondary porosity of the rock mass is fractures. Fractures divide the rock mass into blocks and it is within these fractures the major part of the ground water flow occurs, the flow in the solid rock mass is insignificant. The fracture system can be divided into water-bearing and non water-bearing fractures. Not all fractures are connected to a system and do not contribute to conduct ground water. The fractures void geometry described by parameters introduced in Figure 5.1 below, where aperture, contact area and channelling are the most important ones affecting the hydraulic properties (Hakami 1995).
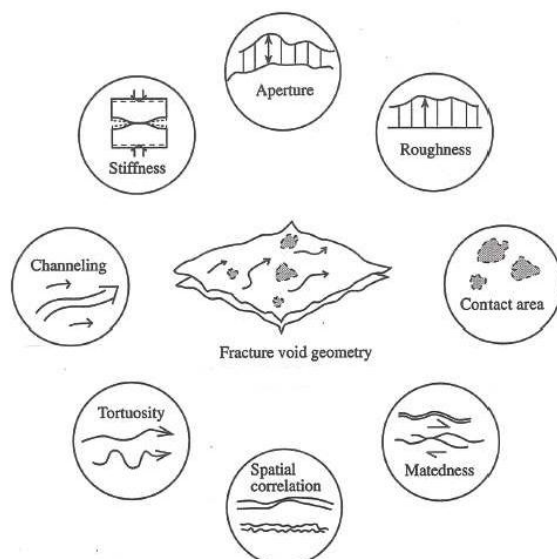

Figure 5.1   Fracture void geometry is determined by parameters where aperture, contact area and channelling are the most influencing on the flow in fractures (Hakami 1995).

Fractures with similar orientations within a limited area usually have the same origin and are categorized in a fracture set. These fractures are often parallel but do not necessarily have the same appearance. They could e.g. differ in hydraulic aperture (Hoobs et al. 1976).

5.1   Excavation damaged zone

When excavating a tunnel, either by TBM (tunnel boring machine) or by drill & blast, the rock closest to the opening is damaged and disturbed, see Figure 5.2. The damaged zone is where old fractures have sheared and opened up. In this zone new fractures may have been created due to the excavation. The damaged zone is irreversible so the deformation will be permanent (Bäckblom 2008).

In the disturbed zone changes of rock properties are negligible but changes of stresses and hydraulic head are apparent. The size of the damaged zone is depending of excavation method. Using the TBM method properties like cutter head design and cutting head forces will affect the appearance of the excavation damage zone. Excavating the tunnel by drill & blast selection of explosives and drilling precision will affect the excavation damage zone. The deformations in the disturbed zone are insignificant or reversible (Bäckblom 2008).

When excavating by TBM the size of the damaged zone could be limited to a few centimetres. In the damaged zone a change of porosity and permeability may occur. Excavating by drill & blast usually gives a larger damaged zone causing a larger change of permeability, especially in the floor where the increase could be up to 2-3 times larger (Rutqvist & Stephansson 2003).
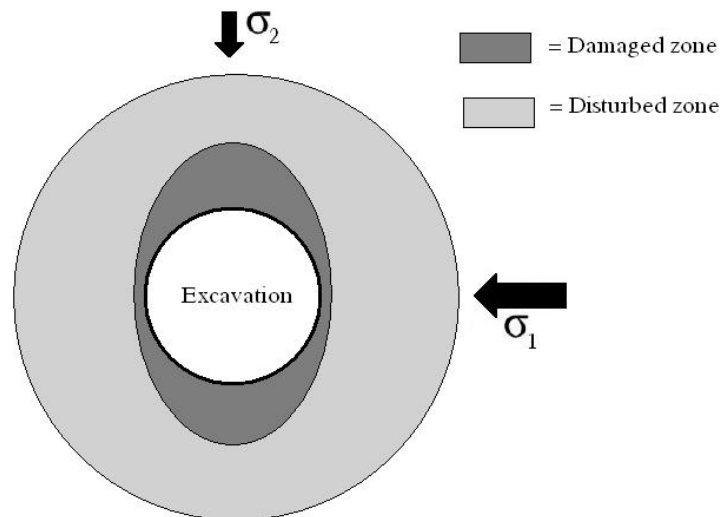

Figure 5.2   Excavation damaged zone and disturbed zone (modified from Bäckblom 2008).

5.2   Fracture deformation

Deformations of a fracture may be caused by changes of both shear stress and normal stress. The normal stress of the fracture is acting perpendicular to the fracture plane. A normal deformation of a fracture is caused by change in normal stress and leads to opening or closure of the fracture perpendicular to the fracture faces. Shear stress is

acting parallel to the fracture plane and normal stress. The shear stresses causing the rock faces to slide along each other, shear deformations. The two kinds of stresses are perpendicular to each other which make the normal stress resisting the shear motions. A change of normal stress may not only lead to opening of fracture due to unloading but also to shear movements (Gothäll 2009). If deformation will be able to take place there must be enough space for the rock to move.

5.2.1 Normal deformation of fractures

The normal deformations could be either reversible or irreversible. Reversible means that the deformation can go back to its initial form whereas the in the irreversible case the deformations are permanent (Bäckblom 2008).

The normal deformation of a fracture, Δu_n, can be expressed:

$$\Delta u_n = \frac{\Delta \sigma_n'}{k_n} \tag{5.1}$$

where $\Delta \sigma_n'$ is the change in effective normal stress and k_n is the fracture normal stiffness (Lindblom 2010). The effective normal stress is expressed as:

$$\sigma_n' = \sigma_n - p \tag{5.2}$$

where σ_n is the normal stress and p is the fluid pressure. When the effective normal stress, σ_n', is increased over a fracture plane there will be normal deformations, Δu_n. An applied normal stress in the fracture will bring the two faces together and crush the rock and new contacts are created, shown in Figure 5.3.
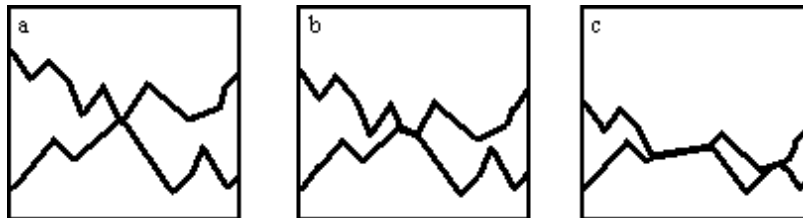

Figure 5.3   Increase in normal stress cause the fracture to deform and the hydraulic and mechanical aperture will decrease (Modified from Gothäll 2009).

A fracture with low normal stress may render in large normal deformations by small applied stress. As a result of increment in effective normal stress the stiffness, k_n, is increased, see Figure 5.4. The rate of normal deformation by applied normal stress is decreased by increased stiffness, equation (5.2). Seen in Figure 5.4 the rate of deformation is largest at small effective normal stress where the stiffness is low. Great effective normal stress will lead to smaller normal deformations due to an increased normal stiffness (Rutqvist & Stephansson 2003).
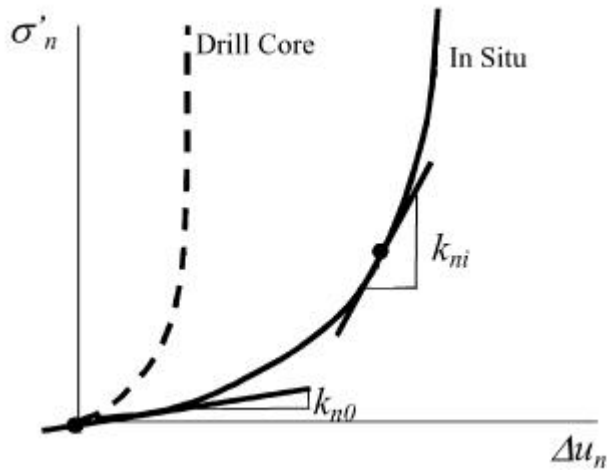
Figure 5.4   Relation between normal deformation of a fracture, Δu_n, and increased normal stress, $\Delta\sigma'_n$, where the inclination of the curve is the fracture stiffness, k_n (Modified from Rutqvist & Stephansson 2003).

When the fluid pressure is increased by grouting and exceeds the normal stress, normal deformation occurs. Equation (5.3) describes an approximate relation between the effective normal stress and fluid pressure when performing grouting:

$$\sigma'_n = \sigma_n - \left(p_w + \frac{\Delta p}{3} \right) \qquad (5.3)$$

where σ'_n is the effective normal stress, σ_n is the normal stress, p_w is the water pressure and Δp is the grouting overpressure. The grouting overpressure profile is described by a cone, and therefore the grouting overpressure is divided by three in order to get an average value. To avoid jacking, when the fluid pressure is equal to the normal stress (effective normal stress is zero), or normal deformation the following condition must be fulfilled (Fransson et al. 2010):

$$\sigma_n > p_w + \frac{\Delta p}{3} \qquad (5.4)$$

5.2.2   Shear deformation of fractures

Shear stresses operate parallel to the fracture plane and perpendicular to the normal stress. The normal stress resists shear movements and when it is decreased it may lead to a normal opening and reduced shear strength. When shear movements occurs the aperture may change due to roughness of the fracture surfaces, see Figure 5.5. The shear movement changes the properties of the fractures; the asperities in the fractures can either be sheared through or overridden (Olsson 1998).
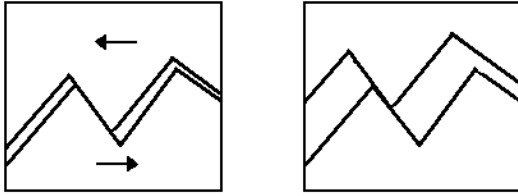
Figure 5.5   Shear stress acting parallel to the fracture causing the fracture to open due to roughness of the fracture surface, the fracture dilates.

When the fracture plane direction deviates from the principal stresses directions there is a risk for shear deformations (when $0° < \alpha < 90°$). Figure 5.6 shows the theories behind shear deformations where σ_1 and σ_2 is the principal stresses, α is the angle between the fracture plane and the largest principal stress, σ_n is the normal stress acting perpendicular to the fracture plane and τ is the shear stress.
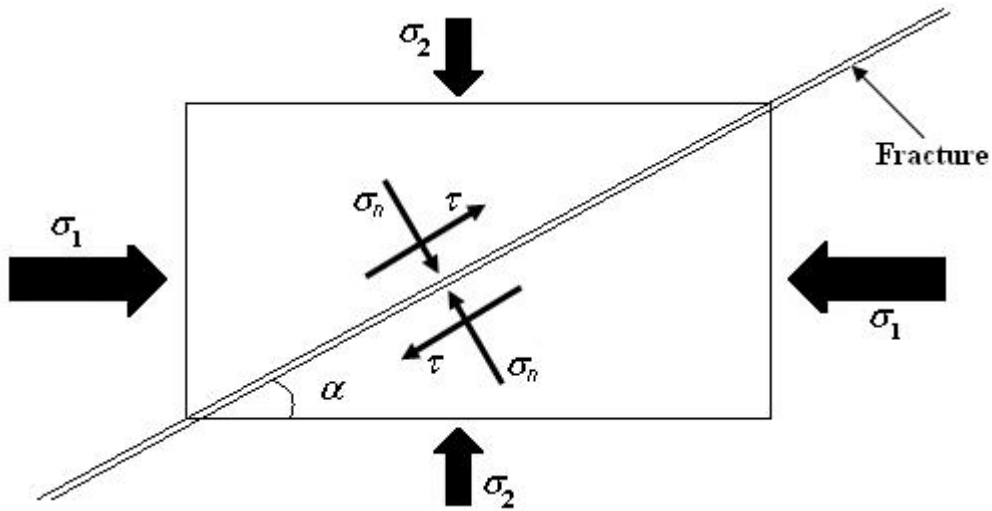

Figure 5.6   Stress equilibrium in a fracture (Gustafson & Fransson 2010).

With help of the horizontal and vertical equilibriums from Figure 5.6 it is possible to express the shear stress and normal stress in principal stresses, equation (5.5) and (5.6):

$$\tau = \frac{\sigma_1 - \sigma_2}{2} \cdot \sin(2\alpha) \qquad (5.5)$$

$$\sigma_n = \frac{\sigma_1 + \sigma_2}{2} - \frac{\sigma_1 - \sigma_2}{2} \cdot \cos(2\alpha) \qquad (5.6)$$

where τ is the fracture shear stress, σ_1 and σ_2 are the principal stresses and α is the angle between the fracture plane and the largest principal stress. The maximum shear stress, τ_{max}, in a fracture before deformation is expressed in equation (5.7):

$$\tau_{max} = \sigma_n \cdot \mu_f \leq \sigma_n \cdot \tan(\phi) \tag{5.7}$$

where σ_n is the normal stress, μ_f is the mobilized friction coefficient and ϕ is the friction angle.

When a fracture is injected of a fluid there will be a fluid pressure, p, acting on the fracture surfaces reducing the normal stress, σ_n, see equation (5.2). The maximum shear stress is affected if the fracture is fluid injected, see equation (5.8):

$$\tau'_{max} = \sigma'_n \cdot \tan(\phi) = (\sigma_n - p) \cdot \tan(\phi) \tag{5.8}$$

where τ'_{max} is the effective maximum shear stress. From equations (5.5), (5.6) and (5.7) it is possible to derive an equation expressing the fluid pressure causing shear deformations, equation (5.9) (Gustafson & Fransson 2010):

$$p_{slip} = \frac{\sigma_1 + \sigma_2}{2} - \frac{\sigma_1 - \sigma_2}{2} \cdot \left[\cos(2\alpha) + \frac{\sin(2\alpha)}{\tan(\phi)} \right] \tag{5.9}$$

6 Grouting

Grouting is a technique used when building underground infrastructure e.g. tunnels and basements. The technique is to seal water bearing fractures to prevent water inflow. In some cases grouting could also be used to increase the bearing capacity in the rock. There are often high demands on grouting. The right agent has to be chosen and that the ground water level should not be lowered too much. It is of high importance that the ground water level will be almost unchanged in urban areas. The demands are higher here and that is because a lower groundwater level could lead to settlements in the ground and many structures could be damaged or destroyed. According to Ellison (2008) a tunnel built today should have a life length of approximately 120 years, so the same demands must be put on the grouting as well. The grouting phase is the phase that takes the longest time in a tunnel building process. It is also an expensive phase and in a non urban tunnel project the grouting costs could be 10-15 % of the total cost. If the tunnel is built in an urban area the grouting cost could rise up to as much as 25 % of the total cost (Ellison 2008).

There are two different types of grouting. Pre-grouting which is used before the tunnel excavation, and post-grouting which is made after the excavation. In some cases both pre- and post-grouting is needed in order to reach the demanded criteria. When doing pre-grouting boreholes are first made into the rock in the same direction as the planned tunnel. The boreholes are made so they create a shield/fan of grouting agent in the rock. After the excavation is made there is a shield/fan protecting the tunnel. This could be seen in Figure 6.1.
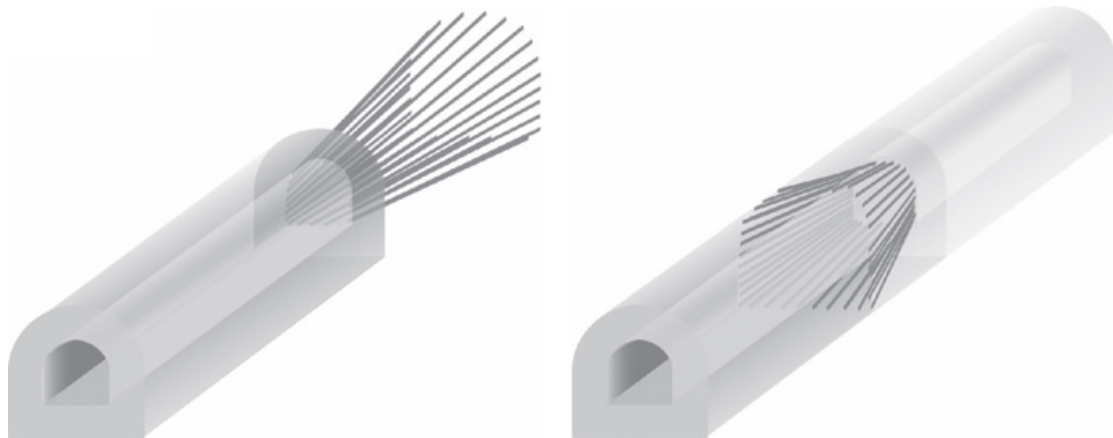

Figure 6.1   The left part of the figure shows a pre-grouting fan performed before excavation, and the right part shows post-grouting made after excavation (Fransson et al. 2010).

One can also mention that the grouting stage of the process is the "weakest link". If the grouting stops for some reason the entire work will stop and that could lead to high costs (Ellison, 2008). It is common with boreholes with a length of 20-25 m and a width of the fan that reaches out 4-5 m from the tunnel walls.

6.1   Grouting design

In grouting there are many parameters of fractures that could affect the grouting efficiency and design. The orientation, aperture and the rock quality are some things that could affect the grouting in one way or another. Some of them are mentioned in this chapter.

According to Houlsby (2006) the spacing of joints is one of the problems. If the joints are widely apart from each other it is easier for the grouting agent to reach out in every single joint. If the joints are close together it can be hard for the grouting agent to reach out in all joints and that could lead to water leakage. This is illustrated in Figure 6.2 below.
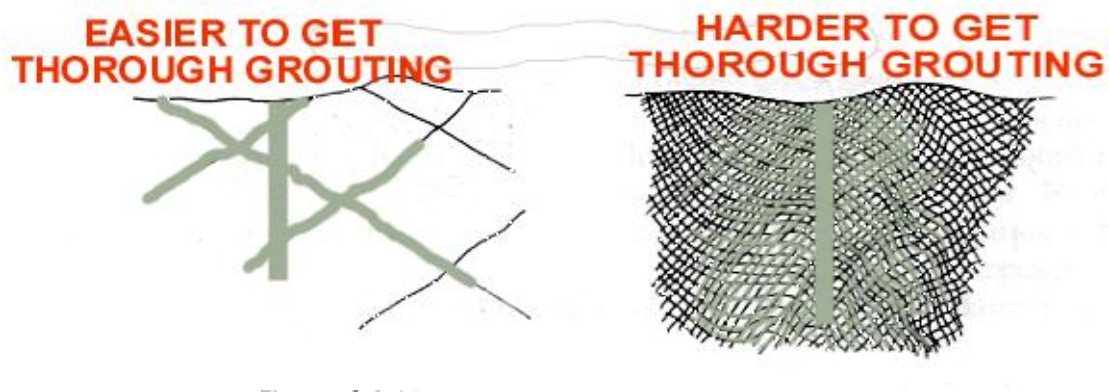

Figure 6.2   The difference of grouting when different spacing between the joints (Houlsby, 2006).

One can easily understand that it is more complicated for the grouting agent to reach out in joints with a smaller aperture than joints with wide aperture. The easiest joints to grout have widths in the range between 0,5 mm and 6 mm. If the joints are to narrow it can be hard for the grouting to reach out. Joints could also be blocked by eroded fragments and such (Houlsby, 2006). Another thing that is of importance is what kind of grouting agent that is used. A cement based grouting agent cannot reach out in as small joints as Silica sol. Silica sols smallest particles are 1000 times smaller than the smallest particles in a cement based grouting agent (Forsman & Funehag, 2004). This is illustrated in Figure 6.3 below:
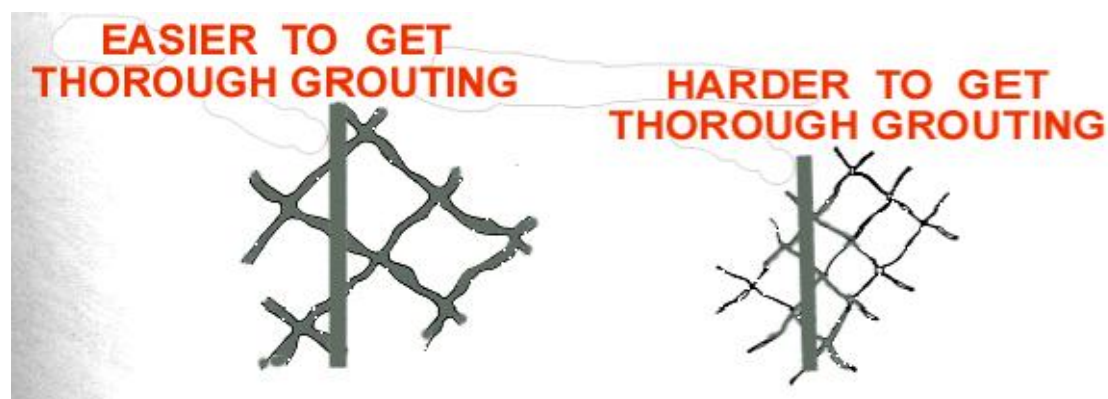

Figure 6.3   Shows how much easier the wider joints is to grout (Houlsby, 2006).

The orientation of the joints is also of importance. A fracture system that has a uniform look need less boreholes and the boreholes that are needed can be made in the same way. If there is an irregular fracture system a lot of boreholes in different directions and lengths can be needed in order to get a good grouting. This automatically leads to a higher cost and more time consuming. This is illustrated in Figure 6.4.
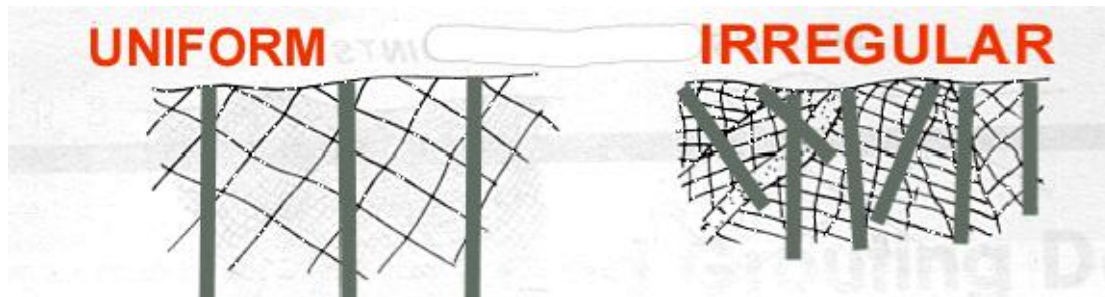

Figure 6.4   Uniform conditions create easier process of drilling and grouting compared with irregular conditions (Houlsby, 2006).

Grouting is a great method for sealing fractures. When the grouting overpressure is higher than the pressure in the surrounding rock it could lead to deformations in the fracture geometry. The grouting pressure reduces the normal stress and changes the relation to shear stresses which may render in shearing movements. The grouting makes the effective vertical stress lower and the small irregularities in the fracture slides upon each other. That makes the fracture wider and more water could pass. It could be the opposite effect as well. If the rock is fragile it could easily be grinded and the small particles could then stuff the fracture so no water could pass at all. It all depends on the rock type, the grouting pressure and the depth which render in vertical stresses (Fransson 2010).

Grouting overpressure, Δp, is a parameter affecting how deep the grouting agent can reach into the joints. Grouting overpressure, Δp, is the grouting pressure, p_g, minus the ground water pressure, p_w, see equation (6.1). The water pressure increases by depth which requires higher grouting pressure to meet the criteria at deeper excavations.

$$\Delta p = p_g - p_w \tag{6.1}$$

It is important that the right grouting pressure is used. Otherwise the rock around the tunnel could be damaged and change its properties. The grouting pressure, p_g, should always be less than the lowest principal stress, σ_3. If the grouting pressure, p_g, is higher than lowest principal stress, σ_3, there could be a deformation of the fracture and that could lead to hydraulic changes in the rock close to the tunnel. Therefore accurate calculations are made before post-grouting (Butrón 2010).

6.2   Grouting agents

There are basically two different types of grouting agents that are used – cement based grouting agent and Silica Sol. The penetration length for the grouting agent can be calculated by equation (6.2). The penetration length, I_{max}, can vary depending on what kind of grouting agent chosen.

$$I_{\max} = \frac{\Delta p \cdot b}{2 \cdot \tau_0}$$
(6.2)

where Δp is the grouting overpressure according to equation (6.1), b is the fracture aperture and τ_0 the yield stress of the grouting agent (Gustafson & Stille 1996)

7 Hydraulic properties

Engineering works in the bedrock such as tunnel excavations, oil and gas extraction, etcetera will have an impact on the in situ stress; an induced stress pattern is created, chapter 4.2. The impacts of the rearranged stresses are mainly shown as deformations in the fractures. This is because the solid rock is stiff and do not deform as easily as the fractures separating the rock into blocks. If the fracture is rough the deformations will change the aperture of the fracture and it may lead to changes of the fluid flow (Olsson & Barton 2001).

To determine the water flow in fractures the cubic law is traditionally used, see equation (7.1).

$$T = \frac{\rho_w \cdot g \cdot b_h^{\,3}}{12\mu_w} \qquad\qquad (7.1)$$

where ρ_w is the density of water, g is the acceleration due to gravity (9.82 m/s² at earth's surface), b_h is the hydraulic aperture and μ_w the fluid viscosity (Snow 1968). The water flow, Q, to a borehole can be obtained from equation (7.2):

$$Q = T \cdot dh \qquad\qquad (7.2)$$

where T is the transmissivity from equation (7.1) and dh is the change of hydraulic head (Fransson 1999). The flows in the fractures are often assumed to laminar. The mechanical aperture is generally determined by measures in 2D when in reality the surface is of course in 3D. The theories behind the cubic law are assuming the two rock faces are flat and parallel. Rock faces are commonly varying in roughness and the aperture differs along the fracture where the two opposing faces have irregular contact areas along the plane. The aperture in the fractures can be divided into different categories; mechanical and hydraulic aperture. The mechanical aperture is the physical opening between the two faces and the hydraulic aperture is described as the gap where the fluid flow occurs (Olsson & Barton 2001).

7.1 Hydromechanical coupling

Fractures in rock can lead to problems. Fracture in combination with water is no exception. The term "hydromechanical coupling" is according to Rutqvist & Stephansson (2003) something that "refers to the physical interaction between hydraulic and mechanical processes. Hydromechanical interactions are common in geological media (e.g., soils and rocks) because such media contain pores and fractures which can be fluid filled and deformable". In general a rock fracture can deform due to a change in the internal pore-fluid pressure or a change in the external load. If there is an increased compressive external load or stress the result could be that the porous medium as a whole could get a smaller bulk volume and a smaller pore volume (Rutqvist & Stephansson 2003). There are two different types of hydromechanical coupling, drained and undrained, but commonly the process is just called direct hydromechanical coupling.

Direct hydromechanical coupling includes four different phenomena, which Rutqvist and Stephansson (2003) explains:

  (i)   A solid-to-fluid coupling that occurs when a change in applied stress produces a change in fluid pressure or fluid mass (e.g. excavation).

  (ii) A fluid-to-solid coupling that occurs when a change in fluid pressure or fluid mass produces a change in the volume of the porous medium (e.g. grouting).

  (iii) A solid-to-fluid coupling that occurs when an applied stress produces a change in hydraulic properties.

  (iv) A fluid-to-solid coupling that occurs when a change in fluid pressure produces a change in mechanical properties.

Process (i) and (ii) are direct couplings through pore volume interactions while process (iii) and (iv) are indirect couplings through changes in material properties, see Figure 7.1.
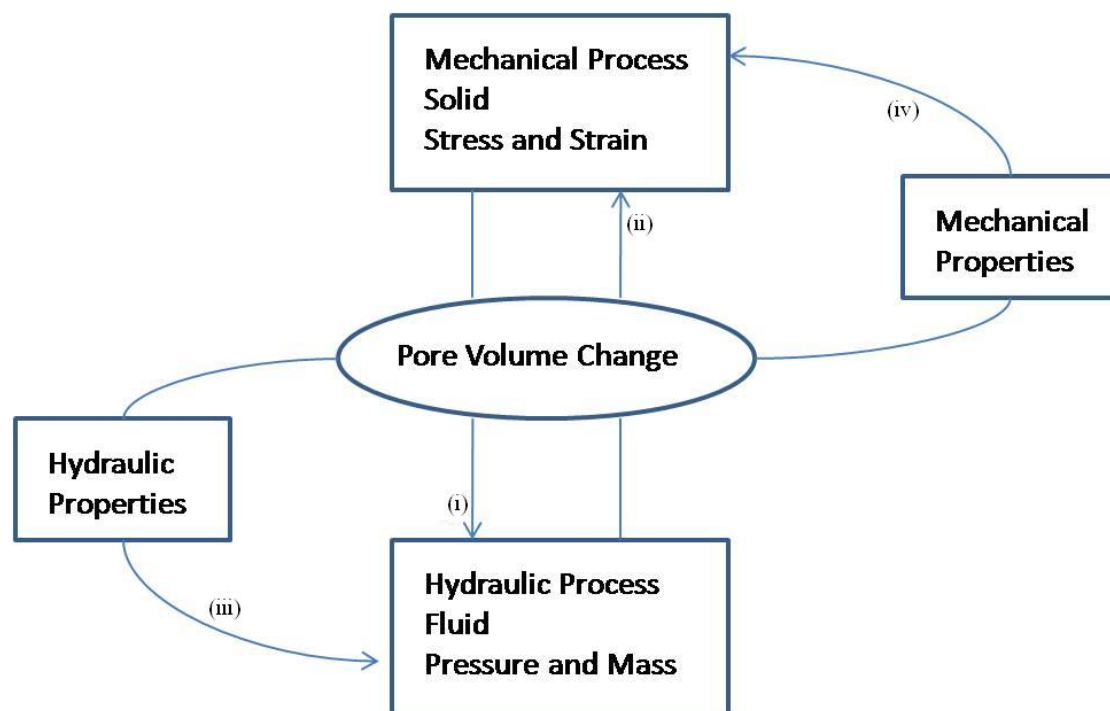

Figure 7.1   *Shows hydromechanical coupling in geological media. (i) and (ii) shows the direct couplings and (iii) and (iv) shows the indirect couplings (Modified from Rutqvist & Stephansson, 2003).*

Both direct and indirect hydromechanical coupling processes may be fully reversible but in some cases fracturing, yielding or fault slip causes irreversibility. Direct hydromechanical coupling occurs in all types of geological media but it tends to be "most important in relatively soft and low-permeability rocks and soils" (Rutqvist & Stephansson 2003). Indirect hydromechanical coupling tend to be most important in fractured rocks or media where changes of permeability is common. A reduction of

the pore volume in process in (i) and (ii) gives a reduction in fluid flow capacity (Rutqvist & Stephansson 2003).

The correlation between fracture stiffness and fluid flow in a single fracture under normal stress is determined by indirect relations. Both the fluid flow and the fracture stiffness have direct relationships to the fracture aperture distribution and contact area. If the fracture stiffness changes it will affect the aperture distribution and the contact areas of the two rock faces. This may lead to impacts on the fluid flow. The rate of fluid flow change in the fracture is greatly determined by the appearance of contact area and the aperture distribution, see Figure 7.2.
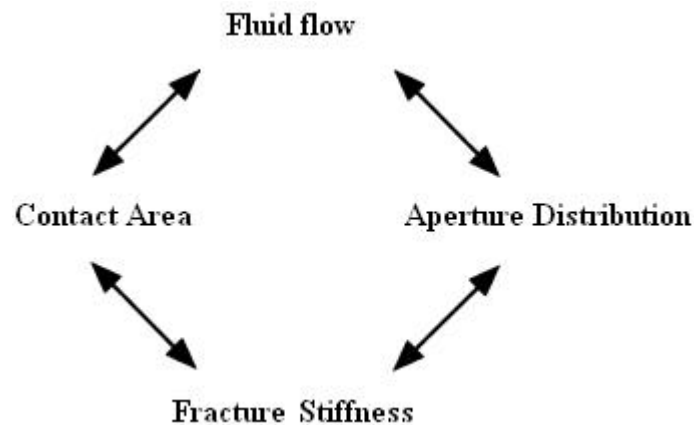

Figure 7.2   Relationship between fluid flow and fracture stiffness in a single fracture. The direct relations (1) – (4) make the fluid flow and fracture stiffness related via aperture distribution and contact area (Modified from Pyrak-Nolte & Morris 2000).

If the aperture distribution is spatially uncorrelated there is likely a great variation in hydraulic aperture and a lot of pathways for the fluid to flow. A change in fracture stiffness would only give minor affect on the fluid flow. An increase in fracture stiffness would render in sealing the smallest hydraulic apertures and an increased contact area of the rock faces. But the pathways with greater hydraulic apertures would not be sealed and still conduct fluid (Pyrak-Nolte & Morris 2000).

In the other case, where the apertures are spatially correlated, a change in fracture stiffness will respond well in fluid flow. Due to correlated hydraulic apertures there will only be a few channels in the fracture conducting fluid and an increment in fracture stiffness will respond well in reduced fluid flow and vice versa (Pyrak-Nolte & Morris 2000).

In Fransson (2009) data from different field experiments have been evaluated to see the relation between hydraulic normal stiffness and hydraulic aperture. The result can be seen in Figure 7.3.
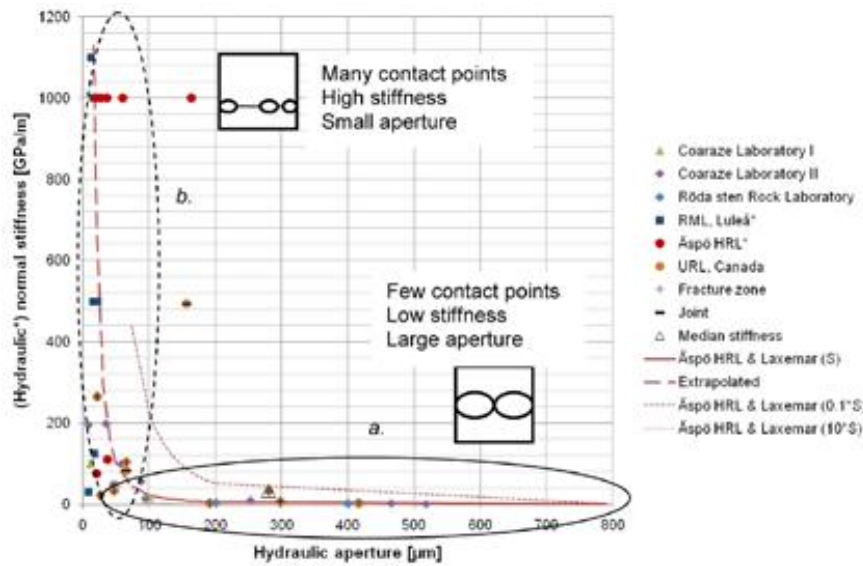
Figure 7.3   Compilation from field data showing relation between normal stiffness and hydraulic aperture. A small change when the normal stiffness is low, within the continuous ellipse, might have a great impact on the hydraulic aperture whereas in the dotted ellipse, with intermediate and high stiffness, large changes of normal stiffness render in minor impact on the hydraulic aperture (Fransson 2009).

According to Fransson (2009) two main tendencies could be seen in the compilation in Figure 7.3:

a) Low stiffness – larger variation in aperture. In this group there is a low effective stress due to e.g. shallow depth. A large fracture normal deformation could be expected.

b) Small apertures – larger variation in stiffness. This could be due to e.g. larger depth. A small fracture normal deformation could be expected.

These data show the great importance of the relation between hydraulic aperture and normal stiffness, mentioned earlier in this chapter.

8 Conceptual model

The following chapter presents the conceptual model that will later be applied to a real case scenario, the TASS-tunnel, to see if the theories can be confirmed or seems plausible.

The development of the conceptual model is based on the theories from chapter 3-7. In Figure 8.1 the two most possible fracture deformations caused by grouting and rearranged stresses due to excavation is shown. The fractures in the cubes in Figure 8.1 are simplified and shows a potential behaviour of the fracture system, the reality are often more complex. The theories is the base for the assumption that the vertical fractures going parallel to the tunnel walls are likely to deform because of reduced normal stiffness when excavating and performing grouting, both pre- and post-grouting.
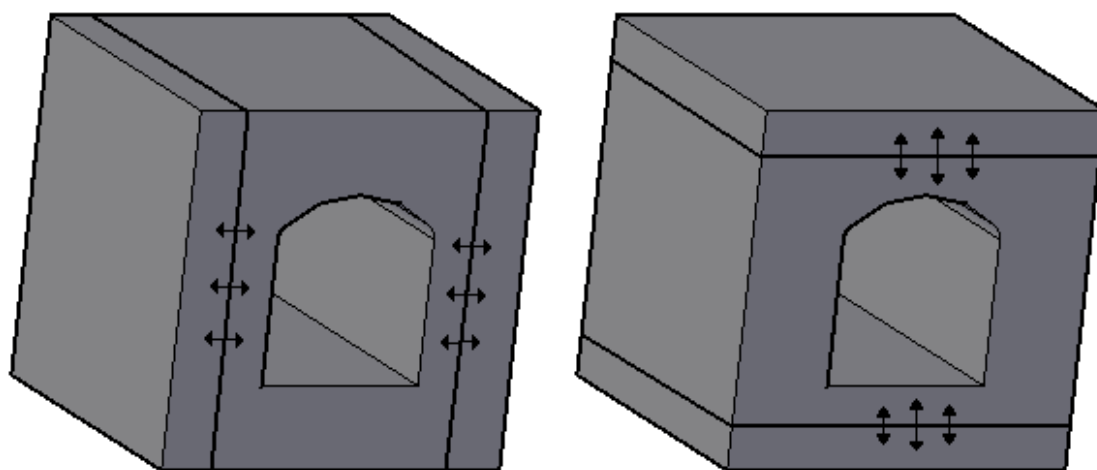

Figure 8.1   Conceptual model of how the fractures close to the excavation are deformed due to grouting and rearranged stresses.

In both cases a deformation of fractures, horizontal and vertical, close to the tunnel leads to opening and closure of fractures. This could lead to rearranged pathways for the ground water flow causing an increased flow in some fractures and decreased in others. The change of ground water flow in a fracture can affect the fracture normal stress which may render in new fracture deformations.

Post-grouting may cause reduced normal stress in fractures which possibly will render in changed hydraulic properties (Fransson & Dahlström in prep., Runslätt & Thörn 2010). Figure 8.2 shows the theories about fracture deformation presented above in a plan view. The red line illustrates a post-grouting borehole intersecting a horizontal fracture, causing a rock deformation. The magnitude of the deformation might be that severe that it can affect the previous performed effect of pre-grouting.
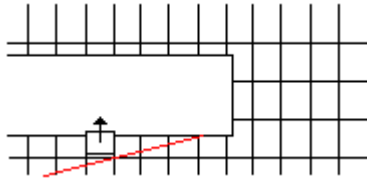
Figure 8.2   Plan view of an excavating with post-grouting which may affect the hydraulic properties and grade of sealing made by pre-grouting.

When excavating the tunnel and the principal stresses are ordered like in Figure 8.3 there is a risk for reduced normal stress in fractures perpendicular to the tunnel direction. This may lead to changes of hydraulic aperture of the fracture due to normal opening or shear movements. When performing pre-grouting in this state of stresses the grouting overpressure reduces the fracture normal stress even further. This is because the smallest principal stress, σ_3, is parallel to the tunnel direction and the other two larger stresses are perpendicular to the tunnel direction and parallel to the fracture, forcing it to open. When the rock is excavated in the tunnel face there is no stress preventing the rock face from bending into the tunnel and open up fractures deeper in the rock.
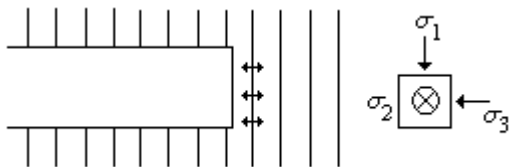

Figure 8.3   Plan view of an excavation indicating that deformation of sub vertical fractures may take place when excavating and pre-grouting the tunnel and the stress directions are arranged as in the figure, with σ_3 running in parallel to the tunnel.

When shearing movement occurs, caused by shear stresses, it will result in new contact areas for the two fracture surfaces. This may lead to change of the hydraulic aperture.

When grouting penetrates fractures and there are shear forces acting in the plane, there is a risk of shear movements. The grouting overpressure, calculated by equation (6.1), changes the fluid pressure in the fracture. The change in fluid pressure affecting the effective normal stress, equation (5.2), which may lead to a decrease in shear stiffness render in shear movements. The roughness of the fracture surfaces may cause the fracture to dilate during shear movements. According to Fransson (2009) there are two possible scenarios, either the asperities will be overridden or they will be sheared through. This may lead to changed hydraulic properties.

Human-induced disturbance, e.g. pre- and post-grouting or underground excavation, may trigger the fracture to further dilation if the permeability correlates to the maximum shear stress direction (Rutqvist & Stephansson 2003).

A description of the conceptual model, used when evaluating the changes of hydraulic properties in the TASS-tunnel due to excavation and grouting, is presented in Table 8.1.

Table 8.1   *Description of the conceptual model of the TASS-tunnel used when evaluating the changes of hydraulic properties due to excavation and grouting (modified from Gustafson 1998).*

Changes of hydraulic properties in the rock close to a tunnel due to excavation and grouting		
Model scope or purpose		
Identify relations between different rock mechanical- and hydraulic properties		
Process description		
Important processes are normal deformation and shear deformation, Kirsch equations, normal stress calculations, shear failure calculations.		
Concepts		**Data**
The tunnel geometry Fracture orientation (sets)	**Geometric framework and parameters**	Area of tunnelsection: ~ 20 m^2 Depth: ~ 450 m Stereonet
Friction angle (ϕ)	**Material properties**	Interval (35°-45°)
Deterministic assignment (fracture sets)	**Spatial assignment method**	All data comes from borehole testing and characterisation
In situ stresses ($\sigma_1, \sigma_2, \sigma_3$)	**Boundary conditions**	Area of interest. With longer distance from tunnel contour the induced stresses approaches the in situ conditions
Computer code used		
MathCAD		
Output parameters		
Tangential and radial stresses in the tunnel wall and critical fluid pressure (slip). Compared to grouting pressure and water pressure (no). effective stress indicates deformation.		

9 Case study TASS-tunnel

The TASS-tunnel is located in the south-east of Sweden at Äspö and SKB:s hard rock laboratory in Oskarshamn. The tunnel is a part of the experiments for testing how the final repository for the spent nuclear fuel should be carried out. SKB:s purpose with the TASS-tunnel is to show that there is enough knowledge to perform a superior sealing of existing fractures, or if needed to develop the method in order to meet the highly set requirements (Funehag 2008, Malmtorp et al. 2009).

9.1 Results from TASS-tunnel

The following chapter is the base when applying the conceptual model on the TASS-tunnel.

9.1.1 Geometry

The almost horizontal tunnel is approximately 80 m long with a section area of nearly 20 m² at a depth of 450 m. The tunnel is 4.2 m wide and 4.8 m high, identical dimensions as the supposed tunnels for the repository of spent nuclear waste. It is located in an area with a relatively low fracture intensity and limited water flow. The dominating rock type in the location of the TASS-tunnel is Äspö diorite. In the pre study phase two core boreholes were made, inside to tunnel contour, in order to evaluate different parameters, e.g. the RQD-value of the rock. Measurements indicate good rock quality with a few exceptions where the fracture intensity was high. The TASS-tunnel direction is 230° which is perpendicular to the largest principal stress, σ_1, and parallel to the smallest principal stress, σ_3 (Funehag 2008, Malmtorp et al. 2009).

Five pre-grouting fans have been made, three of them outside the tunnel contour and two inside the tunnel contour along the tunnel. The first fan is situated at the entrance of the TASS-tunnel at the main tunnel, TASI. According to equation (5.4) the total fluid pressure used was 5.33 MPa. The appearance of the grouting fans can be seen in Figure 9.1 (Funehag 2008). There was also a post-grouting conducted in section 3 in order to measure the in leakage. The post-grouting was divided into two stages, the first one treated the floor/walls and the second the roof.
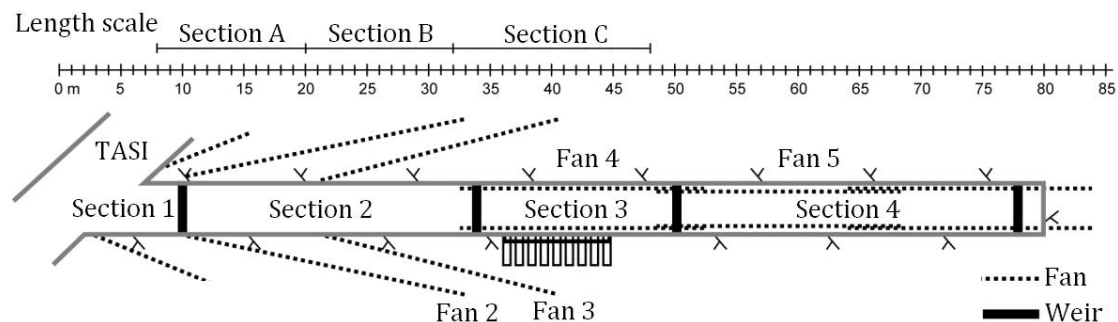

Figure 9.1   *Plan view of the TASS-tunnel including fans, weirs and different sections with the centre of the TASI-tunnel as reference for the length scale. Sections A – C are the stretches where the fracture mapping*

The TASS-tunnel is divided by weirs into four different sections. Approximately 20 m into the tunnel, in section 2, a fracture zone is crossing the tunnel almost perpendicularly. This is a fracture zone is mentioned as 'structure 5' (Hernqvist, Gustafson & Funehag, 2009, Funehag 2008).

Table 9.1 shows a compilation of data, from TASS-tunnel, relevant for further investigations and calculations.

Table 9.1   Table of data from TASS-tunnel (Data collected from Andersson & Martin 2009, Butrón et al. 2010, Funehag 2008 and Malmtorp et al. 2009).

Rock type	Äspödiorite (Funehag 2008)
Tunnel length	80.5 m (Butrón et al. 2010)
Tunnel depth	450 m (Malmtorp et al. 2009)
Area of tunnel section	~20 m^2 (Malmtorp et al. 2009)
Tunnel orientation	230° (Funehag 2008)
Total fluid pressure	5.33 MPa (Equation (5.4))
Injection pressure	10 MPa (Funehag 2008)
Hydraulic apertures	10 -170 µm (Funehag 2008)
Largest principal horizontal stress, σ_H	30 MPa (Andersson & Martin 2009)
Smallest principal horizontal stress, σ_h	10 MPa (Andersson & Martin 2009)
Principal vertical stress, σ_v	15 MPa (Andersson & Martin 2009)
σ_H direction	310° (Malmtorp et al. 2009)

9.1.2   Fractures

The rock quality in the TASS-tunnel area is mainly very high with a few exceptions. For the most of the tunnel stretch the RQD-value is high, higher than 80, but for a few parts of the tunnel the value is lower, about 60. This indicates a good to excellent rock mass quality, but of course fractures still occur.

The 2069 mapped fractures in the three cored boreholes are presented in Figure 9.2. Seen from the fracture rose in Figure 9.2, the main fracture orientation is NW-SE, running perpendicular to the tunnel direction. The largest principal stress, σ_1, has almost the same orientation as the main fracture set (Funehag 2008).
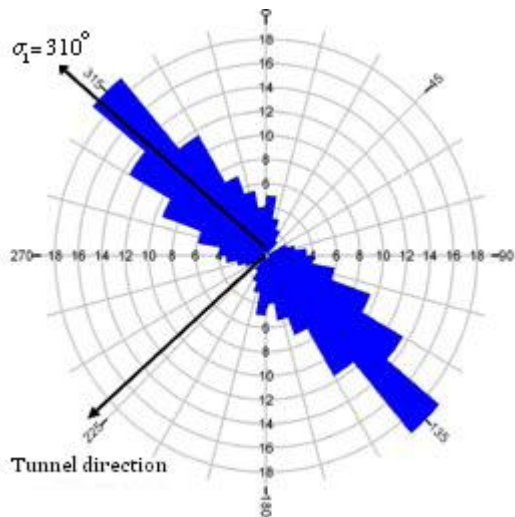
Figure 9.2   Fractures from all three cored boreholes in the TASS-tunnel accumulated in one fracture rose (Modified from Funehag, 2008, pp14).

The excavation was conducted in different steps followed by fracture mapping rendering in three different Schmidt nets for the section 8-48 m, see Figure 9.3, of the tunnel. The section was divided into three different subsections, mentioned A,B and C. Section A represent the fracture mapping for the excavation 8 - 20 m into the tunnel, section B 20 - 32 m and section C 32 - 48 m (Malmtorp et al. 2009)
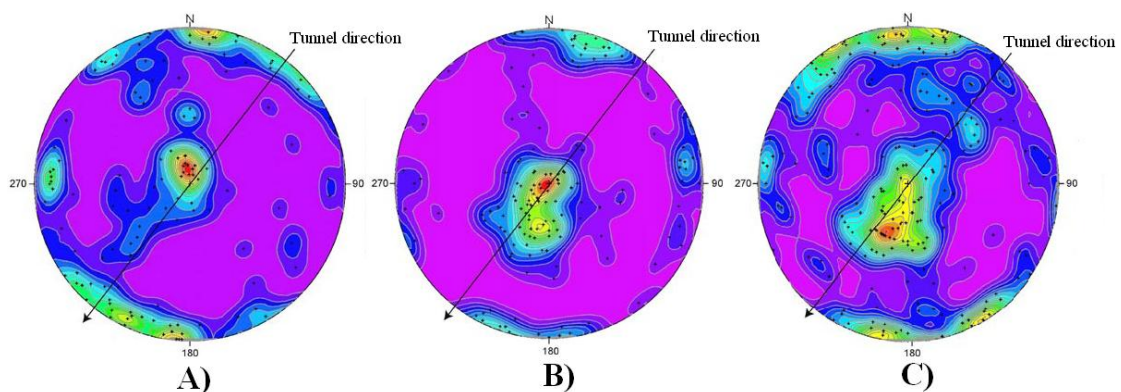

Figure 9.3   Schmidt net of the three evaluated sections of TASS-tunnel. The left one shows section A, the one in the middle section B and the right one section C. Sections A-C is shown in Figure 9.1 (Modified from Malmtorp et al. 2009).

The three Schmidt nets in Figure 9.3 are similar in general with some deviations. The Schmidt nets show that significant horizontal and vertical fracture sets occur. It is easy to see that most of the vertical fractures are perpendicular to the tunnel direction, though the tendency points to deviations of the fracture orientation with increased tunnel length.

According to Talbot & Sirat (2001) the fractures of the Äspö HRL area could be divided into six different sets. Measurements show that 8.3% of the measured fractures in the area were wet. This is assumed to be significant for the entire area, including the TASS-tunnel.
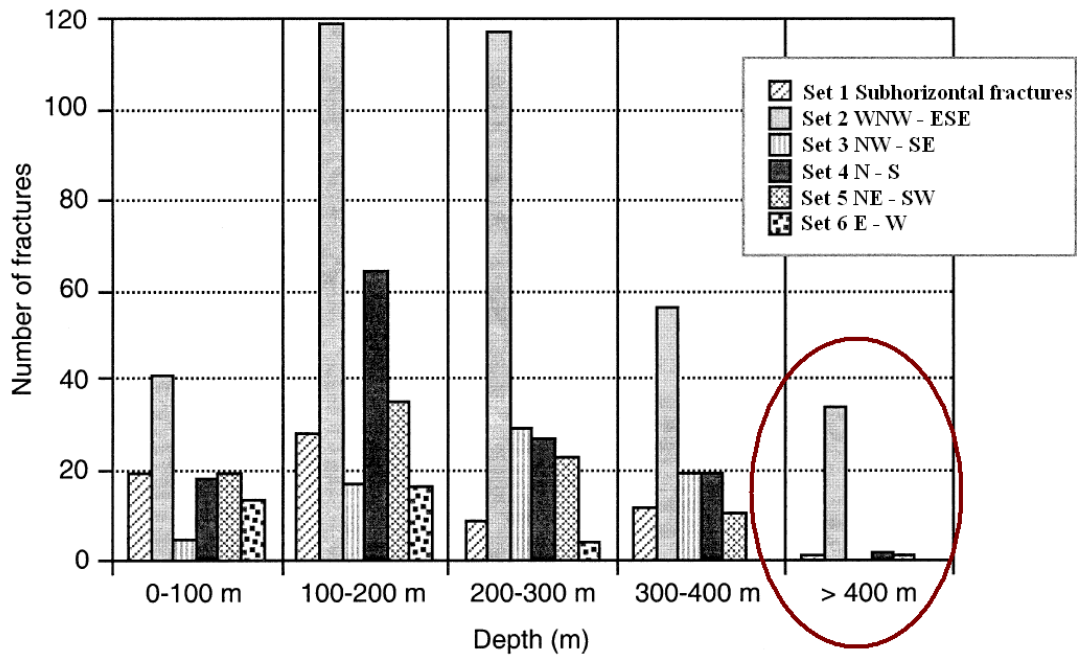
Figure 9.4   *The diagram showing all wet fractures at different depths. The red ellipse shows wet fractures deeper than 400 m which is most essential for the TASS-tunnel. The six bars in each section represent different fracture sets described by the legend in the upper right (Talbot & Sirat, 2001).*

In Figure 9.4 all wet fractures at different depths in Äspö HRL are shown. The six different bars represent the six different sets of fractures, where set 1 is horizontal fractures and set 2-6 are all vertical fractures. Set 2 and 3, represent the NW-SE direction, which is the most frequent fracture set even when it comes to wet fractures. The TASS-tunnel is situated at a depth of 450 m and therefore the last section of the diagram in Figure 9.4, marked with a red circle, is of greatest importance. Even if the number of measured fractures below 400 m is clearly reduced, it is obvious that nearly all of them belong to set 2 (NW-SE orientation).

Figure 9.5 shows all the wet fractures in the TASS-tunnel, presented in a Schmidt net, and the result correlates well with the diagram in Figure 9.4. The Schmidt net clearly shows that most wet fractures that occur in the TASS-tunnel belong to fracture set 2, which means that they are vertical and parallel to the tunnel.
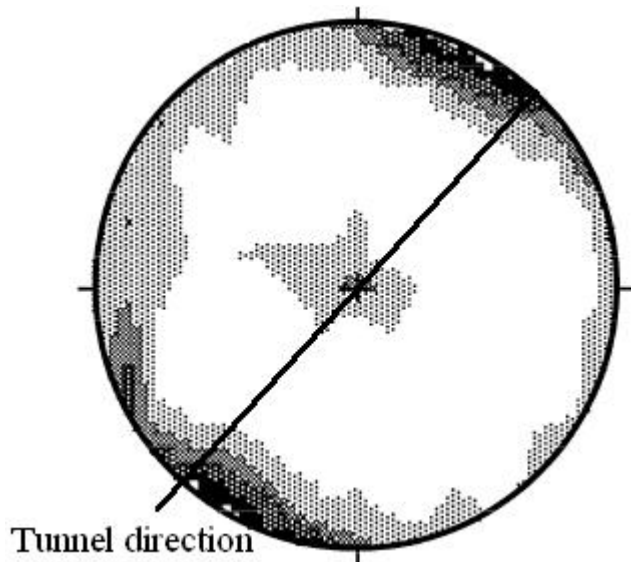
Figure 9.5   Schmidt net of all the wet fractures during excavation in Äspö HRL. Most wet fractures occur in the vertical fracture set going perpendicular to the tunnel front (Modified from Talbot & Sirat 2001).

9.1.3   Stresses

As described in chapter 4.1 the relation of the in situ stresses determines what regime that occurs in the rock and how the fractures are oriented. Figure 9.6, compiled in Talbot & Sirat (2001) shows the regimes by depth at Äspö. At the depth where the TASS-tunnel is situated, at 450 m, there is a strike-slip regime occurring. Data from Andersson & Martin (2009) also proves a strike-slip regime where the largest principal horizontal stress, σ_H, is 30 MPa, the smallest principal horizontal stress, σ_h, is 10 MPa and the principal vertical stress, σ_v, is 15 MPa. It has to be mentioned that the magnitudes of the stresses comes from measurements in the APSE-tunnel, a tunnel at the very same depth as the TASS-tunnel but approximately 150 m apart. Due to the fact that the APSE-tunnel is located close to the TASS-tunnel and at the same depth the stress data from the APSE-tunnel is adoptable for the TASS-tunnel.
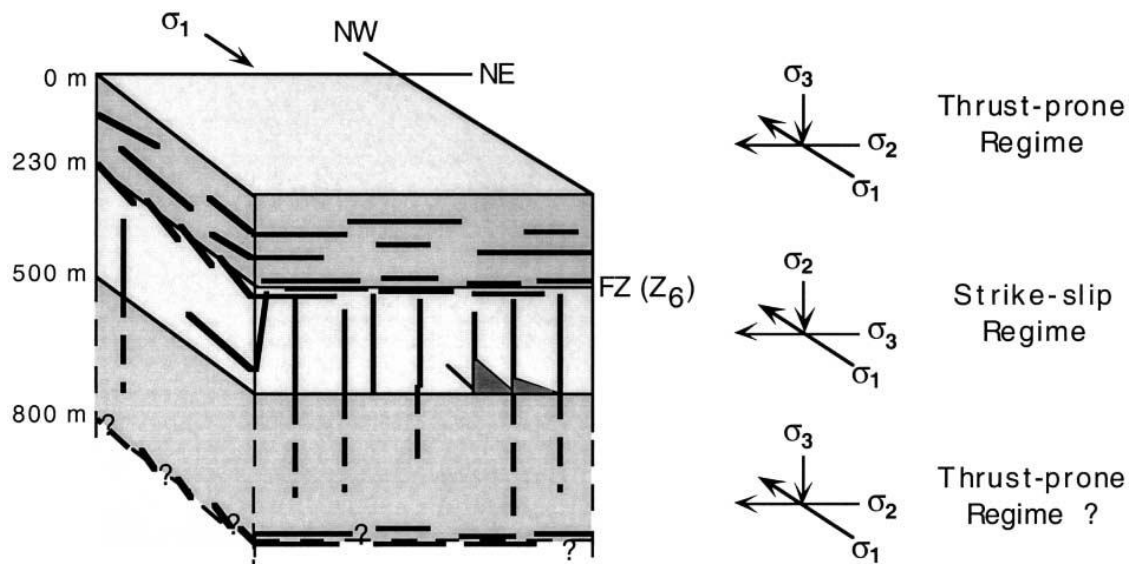
Figure 9.6   The regimes of stresses at Äspö and main orientations of wet fractures by depth (Talbot & Sirat, 2001).

9.1.4   TASS-tunnel inflow data

Drip mapping has been conducted at the TASS-tunnel to study how impermeable a tunnel can get. Simplified it is an identification of how much water that is leaking in to the tunnel after pre grouting and after post grouting. The tunnel was divided into four different stretches separated from each other on the floor by weirs. The four stretches were 10 – 33.8 m, 33.8 – 50 m, 50 – 76.5 m and 76.5 – 80.5 m, see Figure 9.1. The section 33.8 – 50 m is the one used for comparison of inflow after pre- and post-grouting since this section is the only one with available inflow data from both grouting stages (Butrón 2010).

According to Butrón et al. (2010) approximately 70% of the roof measured in the section 10 – 33.8 m was dry, while approximately 90% of the roof in the other sections where dry. One possible reason why the section 10 to 33.8 m was not as dry as the other sections could be due to the fact that a highly transmissive fracture zone crosses the tunnel in this section, mentioned earlier. The fracture zone seemed to give this section more dripping spots than in other sections, although most of them are just moist areas. That is according to Butrón et al. (2010) expected in a fracture zone where the dispersion of the remaining inflow values is small.

Figure 9.7 shows a compilation of the fracture mapping and the drip characterization mapping in TASS tunnel, section 10 to 33.8 m, after pre-grouting and excavation. The orange areas are the ones where dripping occur and it is easy to see that the dripping areas are located along parallel fractures, vertical or horizontal, and in some extent also along the fractures crossing the tunnel.
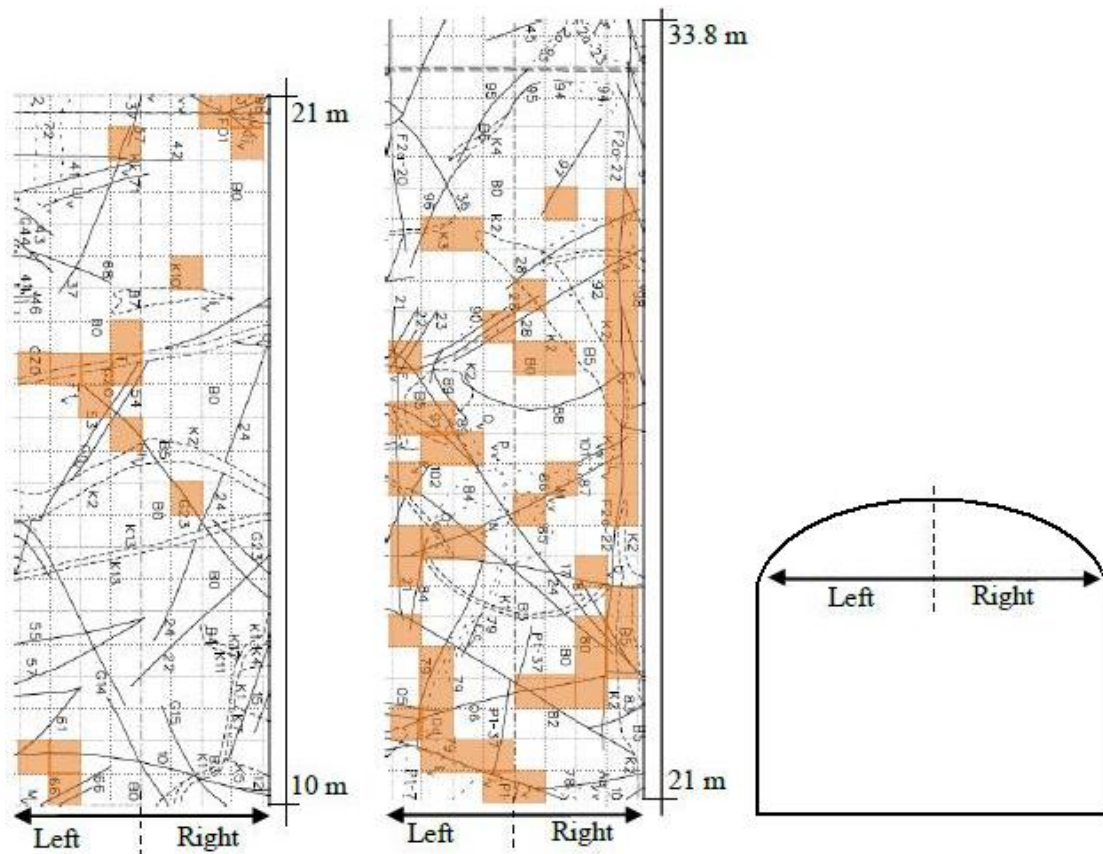
Figure 9.7   Drip and fracture mapping of the roof, after pre-grouting, in section 10 – 33.8 m presented in a plan view. The orange squares indicate non dry areas. To the right in the figure there is a sketch of the tunnel showing what part of the drip mapping corresponds to (Modified from Butrón et al. 2010).

Figure 9.7 shows how many dripping spot that might occur in section 2 which is crossed by a fracture zone after pre-grouting. Figure 9.8, on the other hand, shows section 3 (33.8 – 50m) that has a lower number of dripping spots after pre-grouting. Unfortunately section 3 is the only section with drip data from both pre- and post-grouting, and that is why this section is evaluated. The post-grouting process is divided into two steps; first the walls and floor is post-grouted, and then the roof.
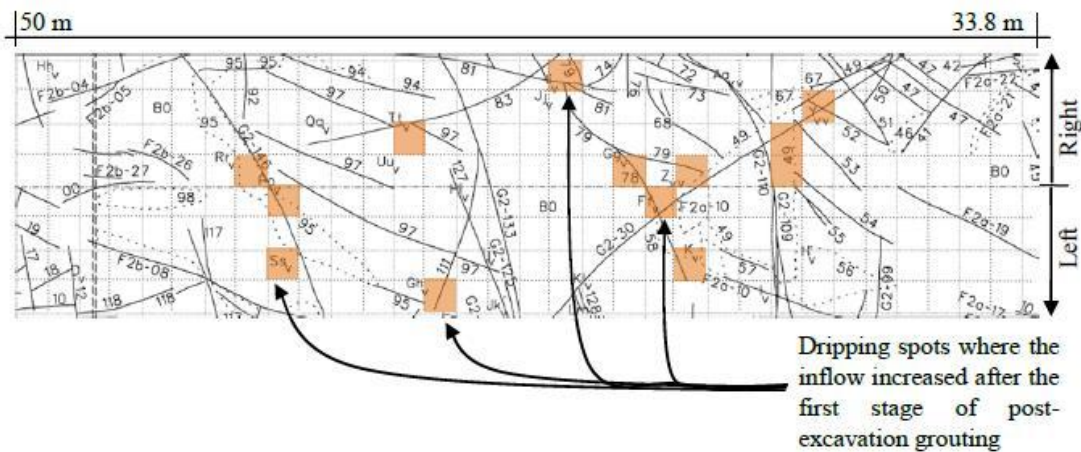
Figure 9.8   *Plan view of fractures and inflow in the roof in section 33.8 – 50 m when pre- and post-grouting have been performed (Butrón et al. 2010).*

The orange squares in Figure 9.8 show areas where inflow occurred after pre-grouting. Four of the 13 wet areas, the areas marked with arrows in Figure 9.8, shows where the inflow increased after the first stage of post-grouting compared to the inflow after pre-grouting.

Figure 9.9 illustrate the 13 wet areas after pre-grouting compared to the inflow after the two post-grouting stages. Every wet area consists of three bars where the yellow one is the inflow after pre-grouting, the red one the inflow after the first post-grouting stage and the blue one the inflow when the second post-grouting stage is completed.

Figure 9.9   *Wet spots in the roof after post-grouting and how the in leakage developed in the different grouting stages (Butrón et al. 2010).*

It is important to notice that Figure 9.9 only shows the in leakage from the roof. There is still a much higher inflow of water from the walls and floor. Despite this the in leakage is much lower after the two post-grouting stages than before. In section 33.8 – 50 m the total in leakage from the roof has lowered from 21 ml/min per 60 m tunnel to 11 ml/min per 60 m tunnel after post-grouting stage 1. The in leakage was further reduced to 8 ml/min per 60 m tunnel by post-grouting stage 2. That is a total reduction of approximately 63% which could be seen as a good result. Like mentioned earlier,

section 33.8 – 50 m is the only section with measured numbers to compare, but the reduction number can probably be used as threshold value for the rest of the tunnel as well (Butrón et al. 2010).

9.2   The conceptual model applied to the TASS-tunnel

First of all it has to be mentioned that the TASS-tunnel is excavated in the most favourable direction in relation to the existing dominant fracture set, see Figure 9.3. This is because perpendicular fractures, crossing the tunnel, minimize the contact area between the fracture and the tunnel, which would be the opposite if the fractures were parallel.

Evaluating the data from chapter 9.1 gives a good understanding of the situation occurring in the TASS-tunnel. The characterization of the principal stresses points to a strike-slip regime, which is also confirmed by Talbot & Sirat (2001). The direction of the main fracture set is vertical, perpendicular to the tunnel direction. Analyses of the Schmidt net, Figure 9.3, also gives a hint that a horizontal fracture set is significant for the TASS-tunnel, although the vertical fracture set is the dominant. A third fracture set, seen in Figure 9.3, worth taken into account consist of vertical fractures parallel to the tunnel, although they are not very common. They could still be of great hydraulic importance because a parallel fracture could be in direct contact for a longer stretch to the tunnel than a fracture crossing the tunnel. Figure 9.10 shows the conceptual model of the TASS-tunnel with inserted fracture sets, principal stresses and tunnel direction.

Figure 9.10   Conceptual model of the TASS-tunnel based on data from the Schmidt net of wet fractures. Two main fracture sets occurs, one vertical and one horizontal (continuous lines). The dotted lines in the conceptual model represents a third fracture set which is not that common but can be of great importance regarding the hydraulic properties. The tunnel direction is 230° and the relations of the principal stresses are shown, indicating a strike-slip regime.

In order to predict potential effects of the hydraulic properties of the fractures close to the TASS-tunnel, the different fracture sets are taken into consideration. The induced stresses (radial- and tangential stresses) are calculated (see Appendix I) by Kirsch equations, chapter 4.2, to be compared to the total fluid pressure. This is to predict potential normal deformation of the fractures introduced in chapter 5.2.1. Shear

deformations are calculated based on the theories from chapter 5.2.2, in order to see where slip failure in fractures occurs (Gustafson & Fransson 2010).

The largest difference between the grouting pressure and groundwater pressure was found in the pre-grouting phase of grouting fan 4. A grouting pressure of 10 MPa was used and groundwater pressure was approximately 3 MPa. According to equation (6.1) this gives a grouting overpressure of 7 MPa. This value is used when calculating the total fluid pressure, which is used when evaluating Figure 9.11, Figure 9.12 and Figure 9.13.

An important remark was the emerging sound from the rock when closing the packer of one of the grouting boreholes. This indicates deformation of fractures caused by water pressure only (Fransson et al. 2010).

It has to be mentioned that the calculations are rough and based on a circular tunnel section. In reality the TASS-tunnel is not circular but this simplification was carried out to easier get an estimation of induced stresses around the tunnel.

Calculations of induced stresses, tangential- and radial stresses, shows that the horizontal fracture set parallel with the TASS-tunnel is not likely to deform due to the total fluid pressure, see Figure 9.11. The radial stress, red line in Figure 9.11, mobilizes quickly by distance in the rock and only fractures situated very close to the tunnel in the roof/floor may be directly deformed. However, this small deformation close to the tunnel may render in indirect deformations further into the rock because the rock is more or less divided into blocks. The tangential stress, blue dotted line in Figure 9.11, is never below the total fluid pressure, green dotted line, indicating that normal deformations of the fractures in the walls are not likely to occur at all.

Figure 9.11   The left part of the figure shows a simplified model of the cross-section of the TASS-tunnel including horizontal fractures. Tangential stresses in the tunnel walls are so high that they are not directly affected by the total fluid pressure, but the radial stresses in the roof/floor might be, where the green line is fallen below. This is shown in the right part of the figure where the total fluid pressure (green crosshatched line), tangential stresses in the walls (blue dotted line) and radial stresses in the floor/roof (red continuous line) are shown with increased radius from the tunnel centre.

Even though vertical parallel fractures are not very common in the TASS-tunnel, they still occur, see Schmidt nets Figure 9.3. They are most common in the latter part of the tunnel. Figure 9.12 shows that vertical fractures parallel to the tunnel walls are the ones most likely to deform due to the total fluid pressure. The radial stress, red line in Figure 9.12 is not mobilizing as quickly as in Figure 9.11 and therefore fractures may be directly affected further away from the tunnel contour compared to the scenario with horizontal fractures. The tangential stress, blue dotted line in the chart, is never below the total fluid pressure and the risk for normal deformation is minimal.
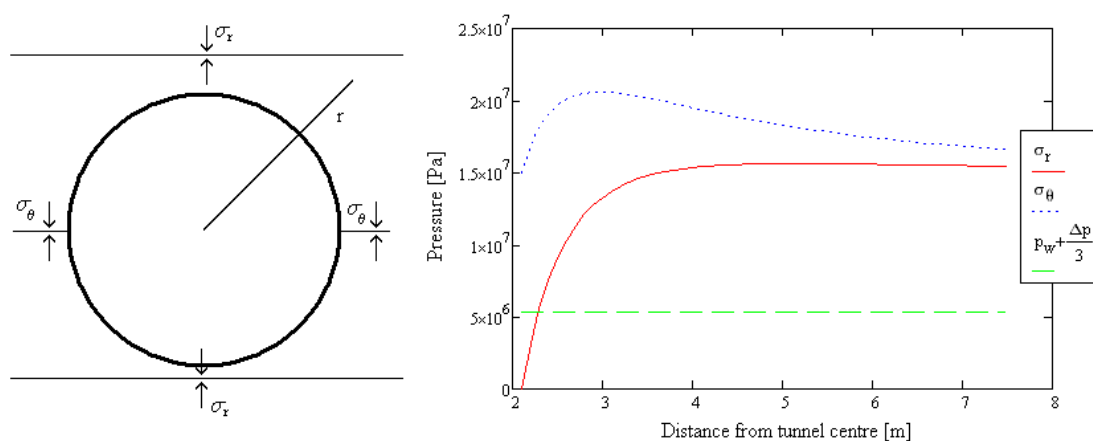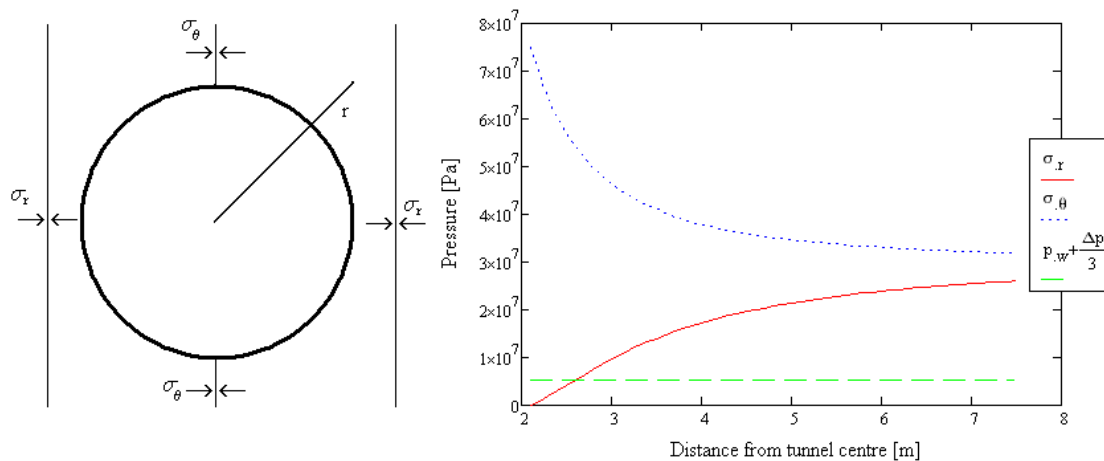

Figure 9.12   The left part of the figure shows a simplified model of the cross-section of the TASS-tunnel including vertical fractures. Tangential stresses in the tunnel floor/roof are so high that they are not directly affected by the total fluid pressure, but the radial stresses in the walls might be. This is shown in the right part of the figure where the total fluid pressure (green crosshatched line), tangential stresses in the roof/floor (blue dotted line) and radial stresses in the walls (red continuous line) are shown with increased radius from the tunnel centre.

The direction of the smallest principal stress, σ_3, correlates with the TASS-tunnel direction. This makes the smallest principal stress, σ_3, the normal stress to the dominating fractures set going perpendicular to the tunnel. Therefore it is possible to assume that the fractures going perpendicular are the ones most likely to normal deform due to grouting, but calculations (see Appendix II) with equation (5.4) proves that the total fluid pressure never exceeds the normal stress. It has to be mentioned that the principal stress σ_3 is set to 10 MPa in the calculations, see Appendix II, but the value might be lower at the tunnel front due to un-loading.

Shear deformation of the fracture sets caused by the total fluid pressure, have been evaluated by using the equations introduced in chapter 5.2.2. All relations between the principal stresses have been assessed but it is only one relation where slip will occur, the one including σ_1 and σ_3. This makes the vertical fractures, going perpendicular to the TASS-tunnel, most exposed to shear deformations caused by the total fluid pressure. The other principal stress relations, σ_1-σ_2 and σ_2-σ_3, never fall below the total fluid pressure and are therefore not likely to slip. These charts and calculations can be seen in Appendix III. It has to be mentioned that these shear deformation calculations are based on a situation when the tunnel is not excavated.
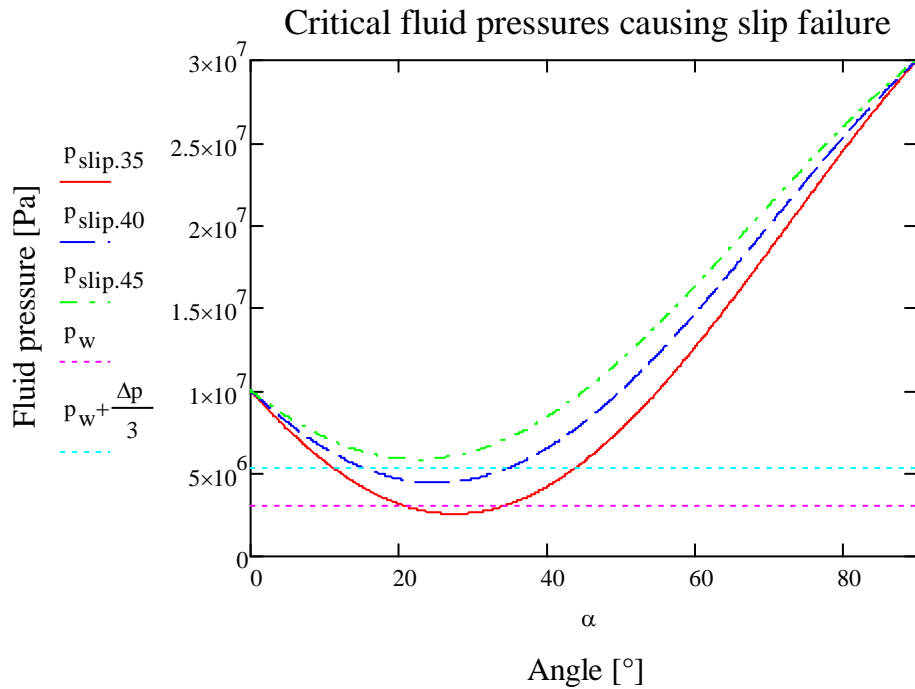
Figure 9.13   *Critical fluid pressures where slip in fractures occurs caused by the principal stresses, σ₁ and σ₃, without any excavation performed. Three typical friction angles, 35°, 40° and 45° (red, blue and green lines) are evaluated. The x-axis shows the angle between the fracture plane and the largest principal stress, σ₁. The horizontal purple line is the total fluid pressure. When the three critical fluid lines fall below the total fluid pressure shear deformation of fractures occur.*

In the TASS-tunnel the largest principal stress, σ_1, is 30 MPa while the smallest principal stress, σ_3, is 10 MPa, rendering in a critical fluid pressure curve between these values. Seen in Figure 9.13 a slip will occur for all the three typical friction angles where α is in the span of approximately 10 – 40°. The red areas in Figure 9.14 are showing the fractures prone to slip due to shear stress. These fractures are vertical and more or less perpendicular to the tunnel direction.
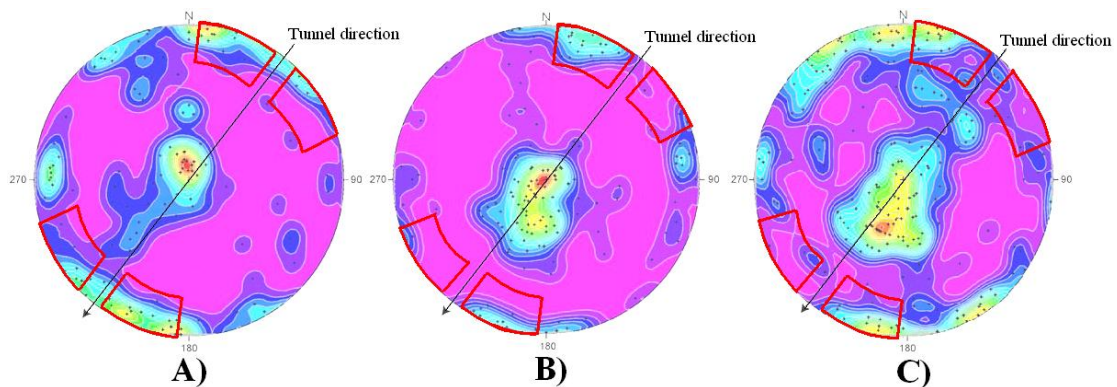

Figure 9.14   *Schmidt net of the tunnel sections A, B and C, see Figure 9.1. The fractures within the red areas, the ones prone to slip, deviate from the largest principal stress direction, 310°, by 10 – 40° and are vertical or*

To summarize expected changes due to grouting, the vertical fractures at high angle to the TASS-tunnel are the ones most likely to deform. The kind of deformation of these fractures that will occur is shear deformation. No other fracture sets are likely to shear deform. Normal deformations will only directly occur in the rock close to the tunnel contour but as mentioned earlier these deformations may cause indirect deformations further into the rock. Fracture set 2 (vertical fractures perpendicular to the tunnel) is, according to Figure 9.4, the fracture set with most wet fractures. The data do not say anything about the hydraulic aperture in the different fracture sets but it is a valid assumption that the fracture set with the most amount of wet fractures carries the highest quantity of water. Since the fractures in set 2 probably carry the highest quantity of water, and are most prone to shear deform, this is where the greatest changes of hydraulic properties will occur. This could lead to opening and closure of water bearing fractures which may force the water into new pathways.

9.2.1 Discussion

Based on our estimates in chapter 9.2 the vertical fractures going perpendicular to the tunnel direction, with a deviation of approximately $10 - 40°$ from the largest principal stress, are most likely to deform. From calculations, compiled in Appendices I-III, only shear deformations is likely to occur in these fractures and is caused by the relation between rock stresses and the total fluid pressure. Small normal deformations will occur in the rock close to the tunnel contour. One reason only small deformations are expected is due to the fact that the tunnel is situated at a large depth with large stresses.

The drip mapping data, from chapter 9.1.4, shows that four spots in section 3 have increased their in leakage from the two post-grouting stages compared to the pre-grouting stage. This could be an indication of deformation of the fractures caused by either normal- or shear deformations, or both. Seen in Figure 9.8 three of the four spots where the dripping increased from the different grouting stages are located along a fracture that is deviating from the largest principal stress, σ_1, with a deviation of 10-40°. It is just one of the four dripping areas, marked with an arrow that is not located along a fracture within the interval above. Despite this, the behavior of the fractures correlates well with the prediction earlier.

According to Butrón et al. (2010) another possible reason why the water inflow increased at some spots in the roof could be due to the excavation damaged zone which may redirect the water from the walls to the roof through linked fractures.

The post-grouting phase was divided into two different stages, where stage 1 was grouting of the walls and floor and stage 2 was grouting of the roof. The reduction of the inflow in the TASS-tunnel roof, seen in Figure 9.9, shows that the in leakage was almost halved after post grouting stage 1 compared to pre-grouting. Although, some spots in the roof did have a higher inflow after post grouting stage 1, see Figure 9.9, and that could indicate a potential rearrangement of the water from the wall and floor into the roof. The total inflow in the roof after grouting stage 2 was almost the same as after stage 1 and that could be an indication of shear deformations of the fractures instead of water rearrangements. The grouting performed in the roof, stage 2, sealed

most of the dripping spots as can be seen in Figure 9.9. The fractures with an unfavorable orientation, approximately 10 – 40° deviation from the largest principal stress, σ_1, are sensitive to changes in fluid pressure, see Figure 9.13 and are likely affected by shear deformations. Therefore the in leakage from post-grouting stage 1 and 2 are quite similar. Some fractures may have been sheared, dilated, and allows more water to pass. On the other hand shear deformations could also render in a decreasing fluid flow but in most deformations in this case we think that the first scenario, with an increased fluid flow, is the most accurate due to the continuous inflow in the roof.

If the tunnel had been situated at a shallower depth, e.g. the Hallandsås tunnel, the result could be different. First of all the principal stresses would be lower and so would the water pressure. Therefore a lower grouting pressure is needed to receive the required grouting overpressure. The grouting penetration length, I_{max}, is depending of depth via the grouting overpressure term, Δp. To achieve the same penetration length in a shallow tunnel compared to a tunnel at a larger depth the grouting overpressure should be the same, see equation (6.2). Though the principal stresses are lower at shallower depth, the grouting overpressure needs to be limited to minimize the risk for deformation, see equation (5.4). The grouting pressure needs to be more accurate calculated in shallower depth to avoid deformations.

With help of different approaches it is possible to predict potential problems in tunnel building. If two of the terms in Figure 9.15 are known, it could be possible to predict the third one. All these terms are connected with each other and could give a valid picture of what would occur. With help of existing data, if it is available, one could make estimations and predictions.

Figure 9.15   Relations between observations, hydraulics and rock mechanics. If two of the parameters are known, it could be possible to predict the last parameter beforehand.

With our knowledge of the hydraulics and rock mechanics a deformation could possibly occur due to the water pressure itself (Figure 9.13), for some specific fracture angles and stress relations. This can be confirmed with the sound that occurred during closing of one packer during a grouting test, mentioned in chapter 9.2.

It is also important to mention that all the assumptions and calculations made of the shear stresses in the TASS-tunnel is based on in-situ stresses. That means that the tunnel itself is not included and affecting the result. One could say that the calculations are applied on "the best case scenario". Therefore it is important to have in mind that the result could differ a bit in real life from the data presented in this report. The calculations of the normal stresses, see Appendix I, are with a tunnel included, but with a circular shape. That is not what the tunnel looks like in real life, but a circular tunnel makes it easier to do principally correct calculations.

The quality of the rock, see chapter 3, can have an impact of how the fractures may deform. A rock with a high RQD-value is less prone to deform then a rock with a low RQD-value. A rock with a low RQD-value often have a greater magnitude of fractures then a rock of higher quality, and that is because the rock with a low RQD-value is less resistant against stresses. Also the type of rock occurring in the tunnel surroundings could be of importance. If e.g. a sedimentary rock is present it is likely to think that fractures will occur in the boundaries between the different layers in the rock and this may render in large hydraulic- and structural problems. To avoid such problems accurate field investigations is needed to be carried out. A good and accurate field investigation could detect potential problems at an early stage and even though an accurate field investigation could cost a lot of money, it is still economically defensible in the long run. If one compares the rock quality between TASS-tunnel and Hallandsås it is possible to see big differences. The rock where the TASS-tunnel is located is a solid rock with few fractures and the tunnel in Hallandsås is situated in a rock that has been unloaded over time, and that is one reason why the rock it is that fractured. The rock and its history are therefore very important to take into consideration. A good knowledge before the tunnel-project begins could therefore give a hint of potential problems.

10 Conclusions

- Fracture deformations, due to excavation and grouting, could have large impact on the hydraulic situation in the rock. Depending on the in situ conditions and the rock quality normal- and/or shear deformations could occur. Input parameters for the analyses could be the friction angle, the in situ stresses, tunnel geometry and the fracture orientation

- Drip data evaluated from the TASS-tunnel correlates fairly well with the theories, about possible hydraulic changes, found in literature. This is also what our calculations point at.

- Based on the in-situ stresses it is the vertical fractures going perpendicular to the tunnel, with a deviation of 10 - 40° from the largest principal stress, which is most likely to deform (shear deformation).

- The relation between hydraulics, rock mechanics and observations could often be used in order to predict possible problems in tunnel building.

- With help of the knowledge, presented in this Master thesis and a few input parameters (e.g. fracture orientation. Friction angle or in situ stresses) it is possible to get a first estimation of potential behaviour in the fractures close to the tunnel.

10.1 Further work

Analyses are made using Kirsch equations and shear failures calculated using in situ stresses. Further analysis using identified fractures sets, tunnel geometry and a numerical tool for estimation of stresses would be interesting.

11 References

Andersson, C. & Martin, C.D. (2009) The Äspö pillar stability experiment: Part I – Experiment design. *International Journal of Rock Mechanics & Mining Sciences*, Vol 46, pp 865-878

Axelsson, M. & Gustafson, G. (2007). Injektering med blaskiga bruk, är det någon idé? *Väg- och vattenbyggaren*, Vol. 4, pp 22-27

Butrón, C., Funehag, J. & Gustafson, G. (2010). How impermeable can a tunnel get? A case study with drip mapping as a method. *Proceedings of the 11th congress of the IAEG – Geologically Active 2010*, pp 2711-2719, Auckland, New Zeeland

Bäckblom, G. (2008). *Excavation damage and disturbance in crystalline rock – results from experiments and analysis.* SKB-report, R-08-08, Swedish Nuclear Fuel and Waste Management Co, Stockholm

Forsman, B. & Funehag, J. (2004). Miljövänligt ämne tätar Hallandsåstunneln. (Electronic) Available: <http://www.miljoportalen.se/mark> (2010-04-23)

Fransson, Å. (1999). *Grouting predictions based on hydraulic tests of short duration: Analytical, numerical and experimental approaches.* Licentiate Thesis, Department of Geology, Chalmers University of Technology, Göteborg, Sweden

Fransson, Å. (2009). *Literature survey: Relations between stress change, deformation and transmissivity for fractures and deformation zones based on in situ investigations.* SKB-report, R-09-13, Swedish Nuclear Fuel and Waste Management Co, Stockholm

Fransson, Å. & Dahlström, L-O. (In prep). *Tunnelframdriftens inverkan på förinjekteringens tätande funktion och injekteringsskärmens utformning med hänsyn till geologi, hydrogeologi and geomekanik.*

Fransson, Å., Tsang, C.-F., Rutqvist, J. & Gustafson, G. (2010). Estimation of deformation and stiffness of fractures close to tunnels using data from single-hole hydraulic testing and grouting. *International Journal of Rock Mechanics & Mining Sciences*, Vol 47, pp 887-893

Funehag, J. (2008). *Injektering av TASS-tunneln. Delresultat t om September 2008.* SKB-report, R-08-123, Swedish Nuclear Fuel and Waste Managment Co, Stockholm

Goodman, R.E. (1993). *Engineering Geology – Rock in engineering construction*, New York.

Gotthäll, R. (2009). *Behaviour of Rock Fractures under Grout Pressure Loadings.* Doctoral Thesis. Division of Soil and Rock Mechanics, Royal Institute of Technology, Stockholm, Sweden

Gustafson, G. & Fransson, Å. (2010). Technical note. *Shear failure in fracture.* Division of GeoEngineering, Chalmers University of Technology, Göteborg, Sweden

Gustafson, G. & Stille, H. (1996). Prediction of Groutability from Grout Properties and Hydrogeological Data. *Tunneling and Underground Space Technology.* Vol 11, No 3, pp 325-332

Gustafson, G. (1998). Structure and use of conceptual models in the ÄSPÖ site investigations. SKB-report, TR-98-10, Chalmers University of Technology, Sweden.

Hakami, E. (1995). *Aperture distribution of rock fractures.* Doctoral Thesis, Division of Engineering Geology, Department of Civil and Environmental Engineering, Royal Institute of Technology. Stockholm, Sweden

Hernqvist, L. (2009). *Characterization of the Fracture system in hard Rock for Tunnel Grouting.* Licentiate Thesis, Division of GeoEngineering, Chalmers University of Technology, Göteborg, Sweden

Hernqvist, L., Gustafson, G. & Funehag J. (2009). Analysis of the transmissivity development during the successive stages of pre-grouting of a tunnel in hard rock. *Nordic Symposium of Rock Grouting* , pp 75-92, Helsinki, Finland

Hoek, E., Brown, E.T. (1984). *Underground Excavation In Rock.* Institution of Mining and Metallurgy, London, UK

Hobbs, B E., Means, W D. & Williams, P F. (1976). *An outline of structural geology.* John Wiley & Sons, Inc. New York, USA

Houlsby, A.C. (2006). Rockgrout: Adapting grouting to suit the geology. (Electronic) Available: <http://users.tpg.com.au/houlsby1/Geol.htm> (2010-04-23)

Kirsch, G. (1898). Die Theorie der Elastizität und die Bedürfnisse der Festigkeitslehre. *Zeitschrift des Vereines deutscher Ingenieure,* Vol 42, pp 797-807

Lindblom, U. (2010). *Bergbyggnad*, Liber, Stockholm

Malmtorp, J., Andersson, C. & Karlzén, R. (2009). *Berguttag I TASS-tunneln. Delresultat t om September 2008.* SKB-report, R-08-122, Swedish Nuclear Fuel and Waste Management Co, Stockholm

Martin, C.D., Kaiser, P.K. & Christiansson, R. (2003). Stress instability and design of underground excavations. *International Journal of Rock Mechanics & Mining Sciences,* Vol 40, pp 1027-1047

Nelson, S.A. (2003). Lecture notes about Sedimentary rock, Tulane University. (Electronical). Available: <http://www.tulane.edu/~sanelson/geol111/sedrx.htm> (2010-02-22)

Olsson, R. (1998). *Mechanical and hydromechanical behaviour of hard rock joints: A laboratory study.* Doctoral Thesis. Chalmers University of Technology, Göteborg, Sweden

Olsson, R. & Barton, N. (2001). An improved model for hydromechanical coupling during shearing of rock joints. *International Journal of Rock Mechanics & Mining Sciences*, Vol 38, pp 317-329

Pyrak-Nolte, L.J. & Morris, J.P. (2000). Single fractures under normal stress: The relation between fracture specific stiffness and fluid flow. *International Journal of Rock Mechanics & Mining Sciences*, Vol 37, pp 245-262

Rhén, I., Follin, S. & Hermanson, J. (2003). *Hydrogeological Site Descriptive Model – a strategy for its development during Site Investigations*. SKB R-03-08. Svensk Kärnbränslehantering AB, Stockholm

Runslätt, E. & Thörn, J. (2010). *Fracture deformation when grouting in hard rock*. Master thesis, Division of GeoEngineering, Chalmers University of Technology, Göteborg, Sweden

Rutqvist, J. & Stephansson, O. (2003). The role of hydromechanical coupling in fractured rock engineering. *Hydrogeology Journal,* Vol 11, pp 7-40

Schindler, A., Jurado M-J. & Müller, B. (1998). Stress orientation and tectonic regime in the northwestern Valencia Trough from borehole data. *Tectonophysics,* Vol 300, pp 63-77

Sibson, R.H. (2004). Controls on maximum fluid overpressure defining conditions for mesozonal mineralisation. *Journal of Structural Geology*, Vol 26, pp 1127-1136

Snow, D.T. (1968). Rock fracture spacing, opening and porosities. *Proceedings of the American Society of Civil Engineers*, Vol 94, pp 73-79

Talbot, C.J. & Sirat M. (2001). Stress control of hydraulic conductivity in fracture-saturated Swedish bedrock. *Engineering geology,* Vol 61, pp 145-153

Oral references

Butrón, C. (2010). Supervising (2010-09-24)

Ellison, T. (2008). Interview (2008-02-18)

Fransson, Å. (2010), Supervising

Gustafson, G.(2008). Lecture in course: *Modelling and problem solving in civil engineering*, (August 2008)

List of appendices

Appendix I:

Normal stress calculations around a circular opening

The rock stresses around the TASS-tunnel have been calculated by Kirsch equations:

$$\sigma_r = \frac{1}{2}\sigma_z\left[(1+k)\left(1-\frac{a^2}{r^2}\right)+(1-k)\left(1-4\frac{a^2}{r^2}+3\frac{a^4}{r^4}\right)\cos(2\theta)\right]$$

$$\sigma_\theta = \frac{1}{2}\sigma_z\left[(1+k)\left(1+\frac{a^2}{r^2}\right)-(1-k)\left(1+3\frac{a^4}{r^4}\right)\cos(2\theta)\right]$$

$$\tau_{r\theta} = \frac{1}{2}\sigma_z\left[-(1-k)\left(1+2\frac{a^2}{r^2}-3\frac{a^4}{r^4}\right)\sin(2\theta)\right]$$

where k is the ratio of horizontal stress and vertical stress (σ_x/σ_z), σ_r is the radial stress, σ_θ is the tangential stress, $\tau_{r\theta}$ is the shear stress, θ is the angle between the vertical centre line and the concerned point, a is the radius of the opening and r is the radius to the centre of the opening. In the TASS-tunnel case σ_1 corresponds to σ_x and σ_2 corresponds to σ_z. The induced stresses calculated by Kirsch equations are later compared to the total fluid pressure achieved when performing grouting.

Inputs:

$\sigma_1 := 30\text{MPa}$

$\sigma_2 := 15\text{MPa}$

$p_w := 3 \cdot \text{MPa}$

$a := 2.1\text{m}$

$p_g := 10 \cdot \text{MPa}$

Calculations:

$k := \dfrac{\sigma_1}{\sigma_2} = 2$

$\Delta p := p_g - p_w = 7\,\text{MPa}$

$p_w + \dfrac{\Delta p}{3} = 5.333\text{MPa}$

Table AI.1 *Induced stresses calculated by Kirsch equations at the centre of the tunnel walls (θ=π/2) and at the centre of the floor/roof (θ=π). All the stresses are stated in MPa.*

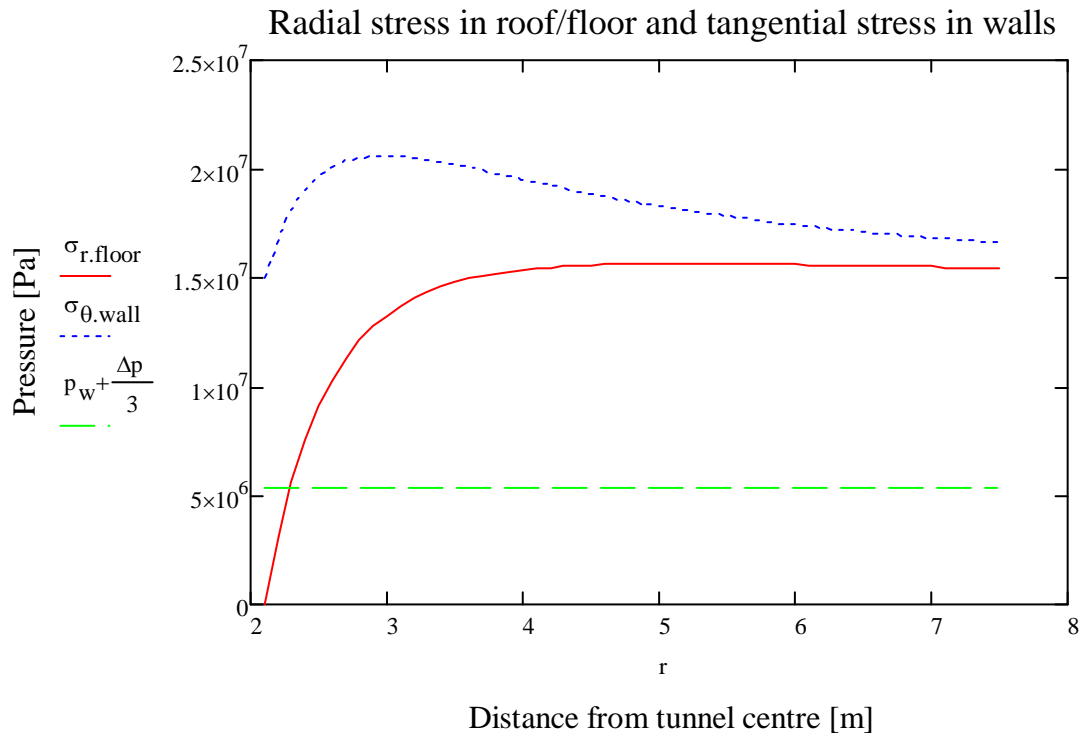| r [m]	θ=π/2		θ=π	
	σ_r	σ_θ	σ_r	σ_θ
2.1	0	15	0	75
2.2	0.84	16.82	3.15	69.18
2.3	1.87	18.12	5.61	64.39
2.4	2.99	19.03	7.55	60.41
2.5	4.15	19.67	9.08	57.07
2.6	5.32	20.10	10.31	54.25
2.7	6.47	20.37	11.30	51.84
2.8	7.58	20.53	12.09	49.77
2.9	8.65	20.61	12.74	47.98
3.0	9.67	20.62	13.27	46.42
3.1	10.64	20.58	13.70	45.06
3.2	11.56	20.51	14.05	43.86
3.3	12.42	20.42	14.34	42.80
3.4	13.24	20.30	14.58	41.85
3.5	14.01	20.18	14.78	41.01
3.6	14.74	20.05	14.94	40.26
3.7	15.42	19.91	15.08	39.58
3.8	16.06	19.77	15.19	38.97
3.9	16.67	19.63	15.28	38.41
4.0	17.23	19.49	15.35	37.91
4.2	18.28	19.21	15.46	37.03
4.4	19.20	18.95	15.54	36.29
4.6	20.03	18.71	15.58	35.66
4.8	20.77	18.48	15.61	35.13
5.0	21.43	18.26	15.62	34.66
5.2	22.03	18.07	15.62	34.26
5.4	22.57	17.88	15.61	33.91
5.6	23.06	17.71	15.60	33.60
5.8	23.50	17.56	15.59	33.33
6.0	23.90	17.41	15.58	33.09
6.2	24.27	17.28	15.56	32.87
6.4	24.60	17.16	15.54	32.68
6.6	24.91	17.04	15.52	32.50
6.8	25.19	16.94	15.51	32.35
7.0	25.45	16.84	15.49	32.20
7.2	25.69	16.75	15.47	32.07
7.4	25.91	16.66	15.45	31.95

Figure AI.1   Induced stresses caused by excavation calculated by Kirsch equations compared to the total fluid pressure when injecting grout.
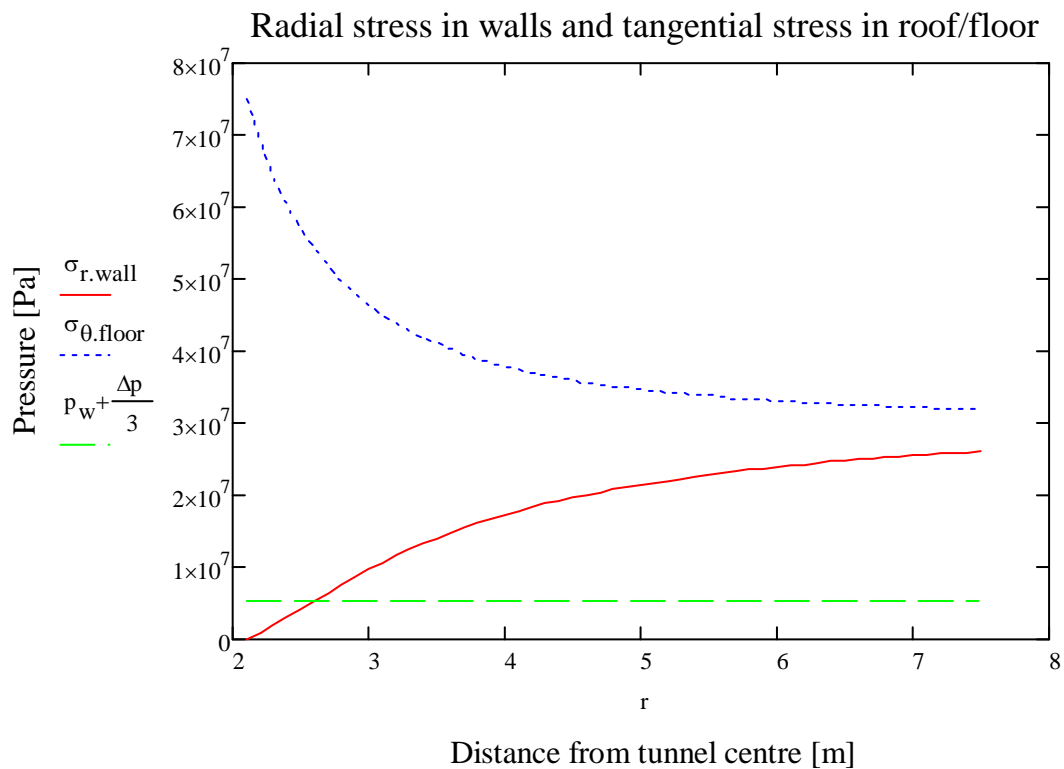

Figure AI.2   Induced stresses caused by excavation calculated by Kirsch equations compared to the total fluid pressure when injecting grout.

Appendix II:

Normal stress calculations in tunnel front due to grouting

This appendix includes calculations of the total fluid pressure when grouting and is compared to the smallest principal stress to see if the fractures perpendicular to tunnel in tunnel are likely to normal deform.

Inputs:

$$\sigma_3 := 10\text{MPa}$$

$$p_w := 3\text{MPa}$$

$$\Delta p := 7\text{MPa}$$

Calculations:

$$\sigma_3 \geq p_w + \frac{\Delta p}{3}$$

$$\text{crit} := p_w + \frac{\Delta p}{3} = 5.333\,\text{MPa}$$
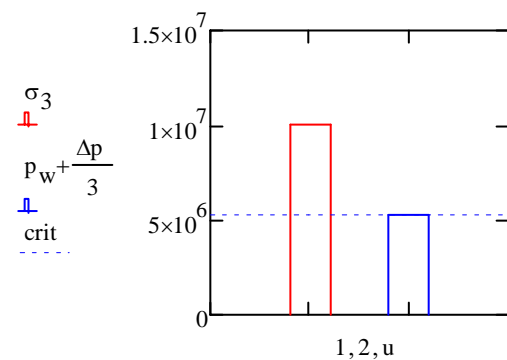

Figure AII.1   Comparison of the smallest principal stress, acting in the TASS-tunnel direction, and the total fluid pressure when performing grouting.

Appendix III:

Shear failure calculations

The calculations below are the in situ stresses, no excavation has been performed.

The critical fluid pressure, p_{slip}, where the fracture will slip for the three different sets of principal stresses can be calculated by:

$$p_{slip} := \frac{\sigma_1 + \sigma_2}{2} - \frac{\sigma_1 - \sigma_2}{2}\left(\cos(2\alpha) + \frac{\sin(2\alpha)}{\tan(\phi)}\right)$$

$$p_{slip} := \frac{\sigma_1 + \sigma_3}{2} - \frac{\sigma_1 - \sigma_3}{2}\left(\cos(2\alpha) + \frac{\sin(2\alpha)}{\tan(\phi)}\right)$$

$$p_{slip} := \frac{\sigma_2 + \sigma_3}{2} - \frac{\sigma_2 - \sigma_3}{2}\left(\cos(2\alpha) + \frac{\sin(2\alpha)}{\tan(\phi)}\right)$$

where σ_1, σ_2 and σ_3 are the principal in situ stresses, α is the angle between the largest of the concerned stresses and the fracture plane, ϕ is the friction angle (Gustafson & Fransson 2010).

Inputs:

$\sigma_1 := 30 \text{MPa}$

$\sigma_2 := 15 \text{MPa}$

$\sigma_3 := 10 \text{MPa}$

$p_w := 3 \cdot \text{MPa}$

$p_g := 10 \cdot \text{MPa}$

Calculations:

$k := \dfrac{\sigma_1}{\sigma_2} = 2$

$\Delta p := p_g - p_w = 7\,\text{MPa}$

$p_w + \dfrac{\Delta p}{3} = 5.333 \text{MPa}$

Table AIII.1   Calculated critical fluid pressures for the three different sets of principal stresses at three different friction angles, 35°, 40° and 45°. The angle, α, is the angel between the fracture plane and the largest of the two involved principal stresses. All the critical fluid pressures are stated in MPa.

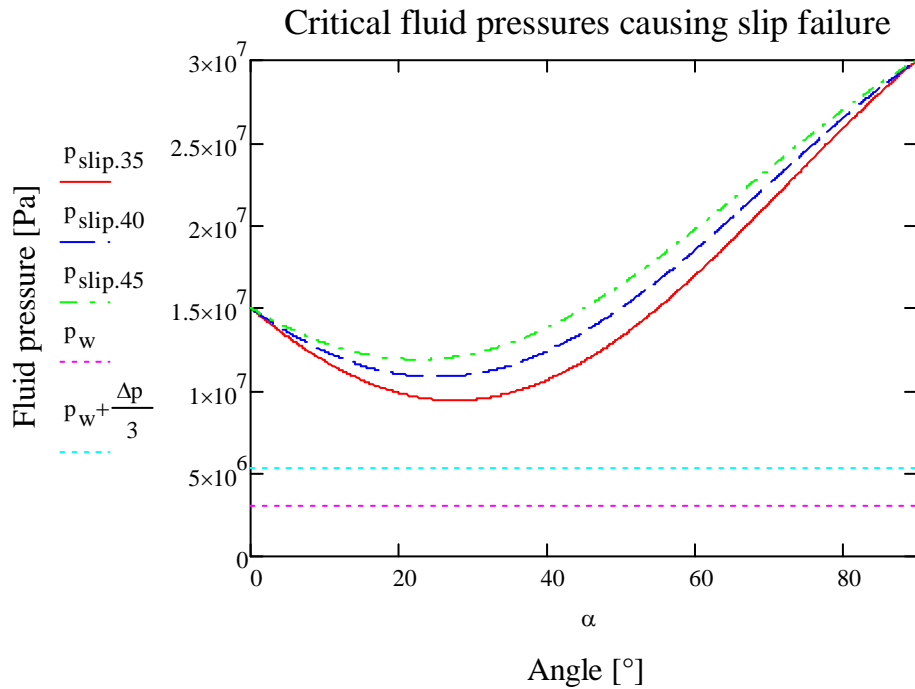| α [°]	σ₁ - σ₂			σ₁ - σ₃			σ₂ - σ₃		
	$p_{slip.35}$	$p_{slip.40}$	$p_{slip.45}$	$p_{slip.35}$	$p_{slip.40}$	$p_{slip.45}$	$p_{slip.35}$	$p_{slip.40}$	$p_{slip.45}$
0	15.00	15.00	15.00	10.00	10.00	10.00	10.00	10.00	10.00
3	13.92	14.10	14.25	8.56	8.80	9.01	9.64	9.70	9.75
6	12.93	13.30	13.60	7.24	7.74	8.14	9.31	9.44	9.54
9	12.05	12.60	13.04	6.07	6.80	7.40	9.02	9.20	9.35
12	11.29	12.01	12.59	5.05	6.01	6.80	8.76	9.00	9.20
15	10.64	11.53	12.25	4.19	5.38	6.34	8.55	8.85	9.09
18	10.13	11.17	12.02	3.51	4.90	6.03	8.38	8.73	9.01
21	9.75	10.94	11.90	3.01	4.59	5.88	8.25	8.65	8.97
24	9.52	10.83	11.90	2.69	4.45	5.88	8.17	8.61	8.97
27	9.42	10.86	12.02	2.56	4.48	6.03	8.14	8.62	9.01
30	9.47	11.00	12.25	2.63	4.67	6.34	8.16	8.67	9.09
33	9.66	11.28	12.59	2.88	5.04	6.80	8.22	8.76	9.20
36	9.99	11.68	13.04	3.32	5.57	7.40	8.33	8.89	9.35
39	10.46	12.19	13.60	3.95	6.26	8.14	8.49	9.07	9.54
42	11.06	12.82	14.25	4.75	7.10	9.01	8.69	9.28	9.75
45	11.78	13.56	15.00	5.71	8.08	10.00	8.93	9.52	10.00
48	12.63	14.39	15.82	6.84	9.19	11.10	9.21	9.80	10.28
51	13.58	15.31	16.72	8.11	10.42	12.30	9.53	10.11	10.57
54	14.63	16.31	17.68	9.50	11.75	13.58	9.88	10.44	10.90
57	15.76	17.38	18.69	11.02	13.18	14.93	10.26	10.80	11.23
60	16.97	18.50	19.75	12.63	14.67	16.34	10.66	11.17	11.59
63	18.24	19.67	20.84	14.32	16.23	17.79	11.08	11.56	11.95
66	19.55	20.87	21.94	16.07	17.83	19.26	11.52	11.96	12.32
69	20.90	22.09	23.05	17.87	19.45	20.74	11.97	12.36	12.69
72	22.27	23.31	24.15	19.69	21.08	22.21	12.42	12.77	13.05
75	23.6	24.52	25.24	21.52	22.70	23.66	12.88	13.18	13.42
78	24.99	25.71	26.30	23.32	24.28	25.07	13.33	13.57	13.77
81	26.32	26.87	27.31	25.09	25.82	26.42	13.77	13.96	14.11
84	27.60	27.97	28.27	26.81	27.30	27.70	14.20	14.33	14.43
87	28.83	29.02	29.17	28.45	28.69	28.90	14.61	14.68	14.73
90	30.00	30.00	30.00	30.00	30.00	30.00	15.00	15.00	15.00

Figure AIII.1 *Critical fluid pressures for fractures affected by σ_1 and σ_2 at three different friction angles, 35°, 40° and 45°. The horizontal dotted lines shows the total fluid pressure before (water pressure, p_w) and after grouting ($p_w + \Delta p/3$).*
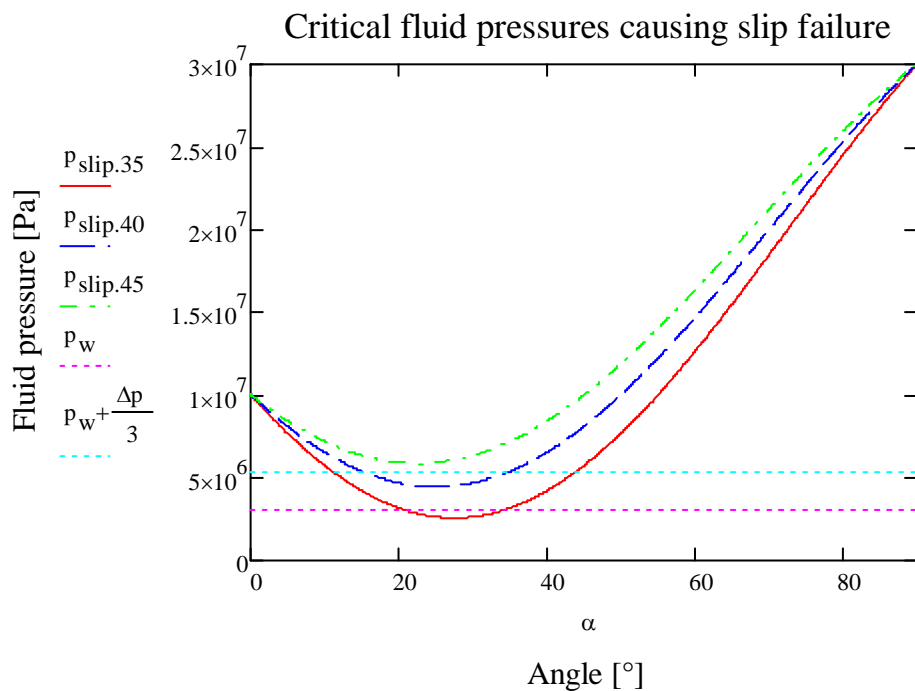

Figure AIII.2 *Critical fluid pressures for fractures affected by σ_1 and σ_3 at three different friction angles, 35°, 40° and 45°. The horizontal dotted lines shows the total fluid pressure before (water pressure, p_w) and after grouting ($p_w + \Delta p/3$).*
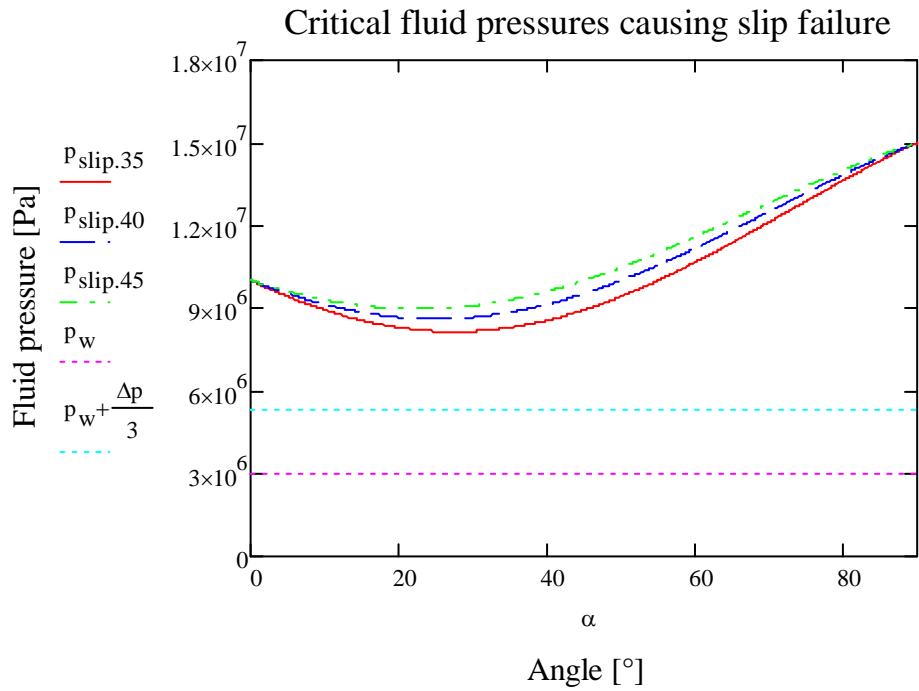
Critical fluid pressures causing slip failure

Figure AIII.3 *Critical fluid pressures for fractures affected by σ_2 and σ_3 at three different friction angles, 35°, 40° and 45°. The horizontal dotted lines shows the total fluid pressure before (water pressure, p_w) and after grouting ($p_w+\Delta p/3$).*